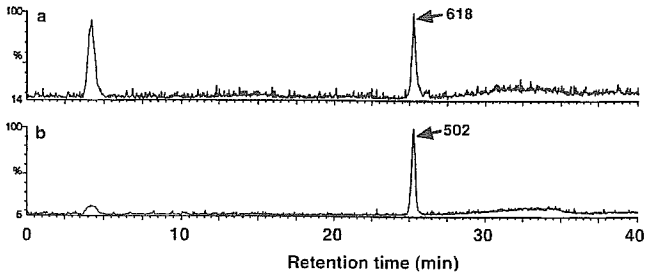

Figure 5. LC-ESI-MS chromatogram of enzymatic hydrolysates of calf thymus DNA reacted with cholyl adenylate. Cholyl adenylate (4 mg) was incubated with DNA (2 mg) at 37 °C, pH 7.0, in 100 mM phosphate buffer. DNA was then recovered from the overnight reaction mixture, followed by enzymatic hydrolysis. (a) Selected ion monitoring at *m/z* 618, which is estimated to be molecular ion of dC modified with cholic acid; (b) selected ion monitoring at *m/z* 502 derived from loss of the deoxyribose moiety from the parent dC-cholic acid adduct with a molecular ion of *m/z* 618.

Scheme 3. Synthesis of N^6-Cholyl-dA

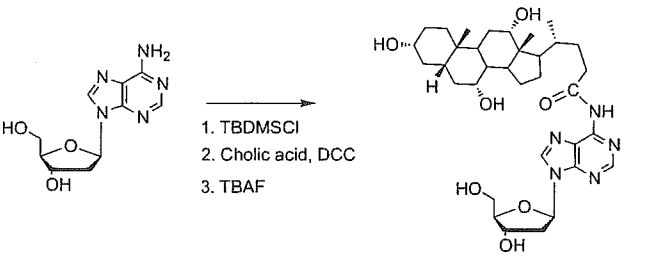

N^6-Cholyl-2'-deoxyadenosine

dC by column chromatography using silica gel. Partially purified silyl-protected dC-cholamide was then treated with 1 M TBAF in THF (Scheme 2). After column separation with ODS, the desired compound was obtained at 20% yield. In a similar manner, dA-cholamide was also obtained at a yield of 7% (Scheme 3); the lower value than for dC is probably due to the lower nucleophilicity of the amino moiety. NMR spectra of these authentic compounds showed diminishing exocyclic NH_2 peaks of dC and dA, whereas new peaks around 10.6−10.7 ppm were observed, confirming introduction of cholic acid at exocyclic amino groups to form amide groups (see Supporting Information of MS spectra of N^4-cholyl-dC and N^6-cholyl-dA). UV absorbance patterns of these synthetic compounds were the same as with reaction products of dC with cholyl adenylate and of dA with cholyl adenylate, respectively. HPLC-MS chromatograms of these compounds were also shown to be identical to those of the products obtained in cholyl adenylate reactions with dC or dA. Therefore, they were concluded to be N^4-cholyl-dC and N^6-cholyl-dA, respectively.

When calf thymus DNA incubated with cholyl adenylate was enzymatically digested and the hydrolysates were applied to LC-MS analyses, LC-MS chromatography clearly showed the presence of a peak of *m/z* 618 accompanied with *m/z* 502, as shown in Figure 5, indicating that N^4-cholyl-dC was formed (see Supporting Information for further information). The yield was around 1.6 adducts per 10^5 nucleosides calculated from the original amount of DNA. In the same reaction mixture, no peak of dA modified with cholic acid (*m/z* 642) was detected under the applied HPLC conditions with the detection limit of around 1 adduct per 10^6 nucleosides (see Supporting Information for an HPLC-UV chromatogram, UV, and full scan MS spectra of N^4-cholyl-dC obtained from the reaction of calf thymus DNA with cholyl adenylate).

Cholyl adenylate has the conjugate acid anhydride moiety arising from carboxylic acid and phosphoric acid. The reaction mechanism thus follows that of a general acid anhydride, which is initiated by the attack of nucleophiles to the carbon atom of the carbonyl group. Reaction of acid anhydride with nucleobases is well-documented for the purpose of protection of functional groups. Generally, nucleophilic substituents such as hydroxyl groups in a deoxyribose moiety and amino groups in a base moiety are targets of acid anhydride. Reactivity of cholyl adenylate with deoxynucleosides, therefore, depends on the nucleophilicity of substrates, resulting in more favorable formation of dC adducts with cholic acid and lesser amounts of the dA adduct as estimated from pK_a values of protonated forms of deoxynucleosides (pK_a = 4.3 for dC and 3.8 for dA) (*26*). Although genotoxicity with bile acids has been reported, the nature of this toxicity is not fully elucidated yet (*12*, 27). Carboxylic acid-acyl adenylates are common intermediates for CoA ester formation, and some have been detected in cells (*13*, *20*, *21*). In vivo, cholyl-CoA itself could provide *N*-cholyl derivatives. Additionally, present studies clearly showed sufficient activity to modify DNA with cholic acid via an acyl adenylate intermediate, indicating a great possible involvement of commonly known acyl adenylates to genotoxicity. The study of in vivo modification of DNA with cholic acid is now being undertaken in our laboratory.

Acknowledgment. This study was supported by a Grant-in-Aid for Cancer Research from the Ministry of Health, Labor, and Welfare, Japan.

Supporting Information Available: MS spectra of N^4-cholyl-dC and N^6-cholyl-dA and HPLC-UV chromatograms, UV spectra, and MS spectra of N^4-cholyl-dC obtained from the reaction of calf thymus DNA with cholyl adenylate. This material is available free of charge via the Internet at http://pubs.acs.org.

References

(1) Setchell, K. D. R., and Russell, D. W. (1994) In *Liver Disease in Children* (Suchy, F. J., Ed.) pp 81−104, Mosby, St. Louis, MO.
(2) Vlahcevic, Z. R., Pandak, W. M., and Stravitz, R. T. (1999) Regulation of bile acid biosynthesis. *Gastroenterol. Clin. North Am. 28*, 1−25.
(3) Chaplin, M. F. (1998) Bile acids, fibre and colon cancer: The story unfolds. *J. R. Soc. Health 118*, 53−61.
(4) Weisburger, J. H., Reddy, B. S., Barnes, W. S., and Wynder, E. L. (1983) Bile acids, but not neutral sterol, are tumor promoters in the colon in man and in rodents. *Environ. Health Perspect. 50*, 101−107.
(5) Reddy, B. S., Watanabe, K., Weisburger, J. H., and Wynder, E. L. (1977) Promoting effect of bile acids in colon carcinogenesis in germ-free and conventional F344 rats. *Cancer Res. 37*, 3238−3242.
(6) Mahmound, N. N., Dannenberg, A. J., Bilinski, R. T., Mestre, J. R., Chadburn, A., Churchill, M., Martuccii, C., and Bertagnolli, M. M. (1999) Administration of an unconjugated bile acid increases duodenal tumors in a murine model of familial adenomatous polyposis. *Carcinogenesis 20*, 299−303.
(7) Imray, C. H., Radley, S., Davis, A., Barker, G., Hendrickse, C. W., Donovan, I. A., Lawson, A. M., Baker, P. R., and Neoptolemos, J. P. (1992) Faecal unconjugated bile acids in patients with colorectal cancer or polyps. *Gut 33*, 1239−1245.
(8) Reddy, B. S., Mastromarino, A., Gustafson, C., Lipkin, M., and Wynder, E. L. (1976) Fecal bile acids and neutral sterols in patients with familial polyposis. *Cancer 38*, 1694−1698.
(9) Scates, D. K., Spigelman, A. D., Phillips, R. K., and Venitt, S. (1997) The use of ^{32}P-postlabeling in studies of the nature and

origin of DNA adducts formed by bile from patients with familial adenomatous polyposis and from normal patients. *Mutat. Res. 378*, 113−125.

(10) Hamada, K., Umemoto, A., Kajikawa, A., Seraj, M. J., and Monden, Y. (1994) In vitro formation of DNA adducts with bile acids. *Carcinogenesis 15*, 1911−1915.

(11) Shibuya, N., Nakadaira, H., Ohta, T., Nakamura, K., Hori, Y., Yamamoto, M., Saitoh, Y., and Ogoshi, K. (1997) Co-mutagenicity of glyco- and tauro-deoxycholic acids in the Ames test. *Mutat. Res. 395*, 1−7.

(12) Glinghammar, B., Inoue, H., and Rafter, J. J. (2002) Deoxycholic acid causes DNA damage in colonic cells with subsequent induction of caspases, *COX-2* promoter activity and the transcription factors NF-kB and AP-1. *Carcinogenesis 23*, 839−845.

(13) Ikegawa, S., Ishikawa, H., Oiwa, H., Nagata, M., Goto, J., Kozaki, T., Gotowda, M., and Asakawa, N. (1991) Characterization of cholyl-adenylate in rat liver microsomes by liquid chromatography/electrospray ionization-mass spectrometry. *Anal. Biochem. 266*, 125−132.

(14) Mano, N., Uchida, M., Okuyama, H., Sasaki, I., Ikegawa, S., and Goto, J. (2001) Simultaneous detection of cholyl adenylate and coenzyme A thioester utilizing liquid chromatography/electrospray ionization mass spectrometry. *Anal. Sci. 17*, 1037−1042.

(15) Goto, J., Nagata, M., Mano, N., Kobayashi, N., Ikegawa, S., and Kiyonami, R. (2001) Bile acid acyl adenylate: a possible intermediate to produce a protein-bound bile acid. *Rapid Commun. Mass Spectrom. 15*, 104−109.

(16) Mano, N., Kasuga, K., Kobayashi, N., and Goto, J. (2004) A nonenzymatic modification of the amino-terminal domain of histone H3 by bile acid acyl adenylate. *J. Biol. Chem. 279*, 55034−55041.

(17) Mihalik, S. J., Steinberg, S. J., Pei, Z., Park, J., Kim, do G., Heinzer, A. K., Dacremont, G., Wanders, R. J., Cuebas, D. A., Smith, K. D., and Watkins, P. A. (2002) Participation of two members of the very long-chain acyl-CoA synthetase family in bile acid synthesis and recycling. *J. Biol. Chem. 277*, 24771−24779.

(18) Steinberg, S. J., Mihalik, S. J., Kim, D. G., Cuebas, D. A., and Watkins, P. A. (2000) The human liver-specific homologue of very long-chain acyl-CoA synthetase is cholate:CoA ligase. *J. Biol. Chem. 275*, 15605−15608.

(19) Solaas, K., Ulvestad, A., Soreide, O., and Kase, B. F. (2000) Subcellular organization of bile acid amidation in human liver: A key issue in regulating the biosynthesis of bile salts. *J. Lipid Res. 41*, 1154−1162.

(20) DeMoss, J. A., Genuth, S. M., and Novelli, G. D. (1956) The enzymatic activation of amino acids via their acyl-adenylate derivatives. *Biochemistry 42*, 325−332.

(21) Mao, L. F., Millington, D. S., and Schulz, H. (1992) Formation of a free acyl adenylate during the activation of 2-propylpentanoic acid. Valproyl-AMP: A novel cellular metabolite of valproic acid. *J. Biol. Chem. 267*, 3143−3146.

(22) Turjman, N., and Nair, P. P. (1981) Nature of tissue-bound lithocholic acid and its implications in the role of bile acids in carcinogenesis. *Cancer Res. 41*, 3761−3763.

(23) Enya, T., Kawanishi, M., Suzuki, H., Matsui, S., and Hisamatsu, Y. (1998) An unusual DNA adduct derived from the powerfully mutagenic environmental contaminant 3-nitrobenzanthrone. *Chem. Res. Toxicol. 11*, 1460−1467.

(24) Ogilvie, K. K. (1973) The *tert*-butyldimethylsilyl group as a protecting group in deoxynucleosides. *Can. J. Chem. 51*, 3799−3807.

(25) Acedo, M., Fàbrega, C., Aviño, A., Goodman, M., Fagan, P., Wemmer, D., and Eritja, R. (1994) A simple method for N-15 labeling of exocyclic amino groups in synthetic oligodeoxynucleotides. *Nucleic Acids Res. 22*, 2982−2989.

(26) Sekine, M., Ohkubo, A., and Seio, K. (2003) Proton-block strategy for the synthesis of oligodeoxynucleotides without base protection, capping reaction, and P−N bond cleavage reaction. *J. Org. Chem. 68*, 5478−5492.

(27) Scates, D. K., Spigelman, A. D., and Venitt, S. (1994) Bile acids do not form adducts when incubated with DNA in vitro. *Carcinogenesis 15*, 2945−2948.

TX050159V

Oncogene (2005) 24, 1328–1337

www.nature.com/onc

Parp-1 deficiency causes an increase of deletion mutations and insertions/rearrangements *in vivo* after treatment with an alkylating agent

Atsushi Shibata[1,2,3], Nobuo Kamada[4], Ken-ichi Masumura[5], Takehiko Nohmi[5], Shizuko Kobayashi[2], Hirobumi Teraoka[3], Hitoshi Nakagama[1], Takashi Sugimura[1], Hiroshi Suzuki[4,6] and Mitsuko Masutani*[,1]

[1]*Biochemistry Division, National Cancer Center Research Institute, Chuo-ku, Tokyo, Japan;* [2]*Kyoritsu College of Pharmacy, Minato-ku, Tokyo, Japan;* [3]*Medical Research Institute, Tokyo Medical and Dental University, Chiyoda-ku, Tokyo, Japan;* [4]*Chugai Pharmaceutical Co. Ltd, Gotemba, Shizuoka, Japan;* [5]*Division of Genetics and Mutagenesis, National Institute of Health Sciences, Setagaya-ku, Tokyo, Japan*

Accumulated evidence suggests that Parp-1 is involved in DNA repair processes, including base excision repair, single-strand and double-strand break repairs. To understand the precise role of Parp-1 in genomic stability *in vivo*, we carried out mutation analysis using *Parp-1* knockout (*Parp-1*$^{-/-}$) mice harboring two marker genes, *gpt* and *red/gam* genes. Spontaneous mutant frequencies of both genes in the bone marrows and livers did not differ significantly between *Parp-1*$^{-/-}$ and *Parp-1*$^{+/+}$ mice ($P > 0.05$). After treatment with an alkylating agent, *N*-nitrosobis(2-hydroxypropyl)amine (BHP), the mutant frequency of the *red/gam* genes in the liver in *Parp-1*$^{-/-}$ mice was 1.6-fold higher than that in *Parp-1*$^{+/+}$ mice ($P < 0.05$). Categorization of the mutations revealed that deletions larger than 1 kb or those accompanying 1–5 bp insertions at the deletion junctions, as well as rearrangements, were more frequently observed in *Parp-1*$^{-/-}$ than in *Parp-1*$^{+/+}$ mice ($P < 0.05$, respectively). In contrast, mutant frequencies of the *gpt* gene in the livers of *Parp-1*$^{-/-}$ and *Parp-1*$^{+/+}$ mice after BHP treatment were both elevated and there was no significant difference between the genotypes. These results indicate that Parp-1 is implicated in suppressing deletion mutations *in vivo*, especially those accompanying small insertions or rearrangements.
Oncogene (2005) **24,** 1328–1337. doi:10.1038/sj.onc.1208289
Published online 20 December 2004

Keywords: Parp-1; *gpt* delta; deletion; mutation; recombination; rearrangement

Introduction

Poly(ADP-ribose) polymerase-1 (Parp-1) is activated by binding to single-strand break (SSB) and double-strand break (DSB) ends, and catalyses polyADP ribosylation of various nuclear proteins, including Parp-1 itself (Yoshihara *et al.*, 1977; Adolph and Song, 1985), histone (Buki *et al.*, 1995), p53 (Wesierska-Gadek *et al.*, 1996), and DNA-dependent protein kinase (DNA-PKcs) (Ariumi *et al.*, 1999) using NAD as a substrate. Parp-1 possesses a BRCT (BRCA1 C-terminal) motif being overlapped with an automodification domain, and binds to various proteins through this domain, including XRCC1 (Masson *et al.*, 1998), histone (Buki *et al.*, 1995), and Parp-2 (Schreiber *et al.*, 2002). Accumulating studies have indicated Parp-1 to be involved in base excision repair (BER) (Caldecott *et al.*, 1996a; Masson *et al.*, 1998), SSB (Okano *et al.*, 2003), and DSB repairs (Morrison *et al.*, 1997) through its enzymatic activity and/or protein–protein interaction through the BRCT domain.

In the BER reaction, cleavage of damaged bases takes place and, subsequently, SSB is introduced by the excision of abasic sites by nucleases. Parp-1 binds to SSB ends and is involved in the recruitment of XRCC1 (Caldecott *et al.*, 1996b; Masson *et al.*, 1998; El-Khamisy *et al.*, 2003), DNA polymerase β (pol β) (Caldecott *et al.*, 1996b; Masson *et al.*, 1998), and DNA ligase III (Leppard *et al.*, 2003). In the cell-free system, DNA polymerization by pol β and strand displacement by flap endonuclease-1 (FEN-1) in the long-patch repair is disturbed in the absence of Parp-1 (Vodenicharov *et al.*, 2000; Prasad *et al.*, 2001). Another study showed a decreased level of long-patch repair in *Parp-1*$^{-/-}$ cells, with reduction in the levels of FEN-1 and DNA ligase I (Sanderson and Lindahl, 2002).

DSB repair is categorized into homologous recombination (HR) repair and nonhomologous end joining (NHEJ) repair pathways. Involvement of Parp-1 in NHEJ repair has been also suggested from the interaction with DNA-PKcs and Ku70/80 (Ariumi *et al.*, 1999; Galande and Kohwi-Shigematsu, 1999). Parp-1 is also indicated to suppress HR repair, and the frequencies of gene-targeting (Waldman and Waldman, 1990; Semionov *et al.*, 1999, 2003; Susse *et al.*, 2004) and sister chromatid exchanges were increased in *Parp-1*$^{-/-}$ cells (de Murcia *et al.*, 1997; Wang *et al.*, 1997) and by treatment with Parp inhibitors (Oikawa *et al.*, 1980).

*Correspondence: M Masutani, Biochemistry Division, National Cancer Center Research Institute, 5-1-1, Chuo-ku, Tokyo, 104-0045 Japan; E-mail: mmasutan@gan2.res.ncc.go.jp
[6]Current address: National Research Center for Protozoan Diseases, Obihiro University of Agriculture and Veterinary Medicine, Obihiro, Hokkaido, Japan
Received 4 May 2004; revised 4 October 2004; accepted 7 October 2004; published online 20 December 2004

The involvement of Parp-1 in BER and DSB repair, and its suppressive role in HR repair, suggests that deletion or insertion mutations may accumulate under *Parp-1* deficiency. On the other hand, it is reported that the gene-targeting frequency was not different between *Parp-1*$^{-/-}$ and *Parp-1*$^{+/+}$ cells, and it is therefore suggested that Parp-1 is dispensable in NHEJ and HR induced by DSBs (Yang *et al.*, 2004).

Analysis of mutant frequencies and spectra in *Parp-1*$^{-/-}$ mice *in vivo* would be helpful to understand the impact of *Parp-1* deficiency on DNA repair and genomic stability. For this purpose, we established *Parp-1*$^{-/-}$ mice, harboring a tandem array of 80 copies of lambda EG10 DNA containing two surrogate marker genes by intercrossing with *gpt* delta transgenic mice (Nohmi *et al.*, 1996). Point mutations can be detected by *gpt* assay, and deletion mutations ranging from 1 bp up to 9.1 kbp are able to be efficiently identified in the *red/gam* genes by Spi$^-$ assay, as shown in Figure 1 (Masumura *et al.*, 1999; Nohmi *et al.*, 1999; Okada *et al.*, 1999).

In the present study, we analysed spontaneous mutations in the bone marrow and livers of *Parp-1*$^{-/-}$ and *Parp-1*$^{+/+}$ mice. Since *Parp-1*$^{-/-}$ mice show higher susceptibility to the lethality induced by alkylating agents (de Murcia *et al.*, 1997; Masutani *et al.*, 2000), and to the tumorigenicity of agents such as *N*-nitrosobis(2-hydroxypropyl)amine (BHP) and azoxymethane (Tsutsumi *et al.*, 2001; Nozaki *et al.*, 2003) compared to *Parp-1*$^{+/+}$ mice, we also analysed mutations after treatment with BHP. We demonstrated that the frequency of deletion mutations, but not point mutations, was higher in BHP-treated *Parp-1*$^{-/-}$ than in *Parp-1*$^{+/+}$ mice ($P<0.05$). Notably, larger size deletions and complex-type deletions accompanying small insertions or recombination/rearrangement were significantly increased in *Parp-1*$^{-/-}$ when compared to *Parp-1*$^{+/+}$ animals ($P<0.05$, respectively).

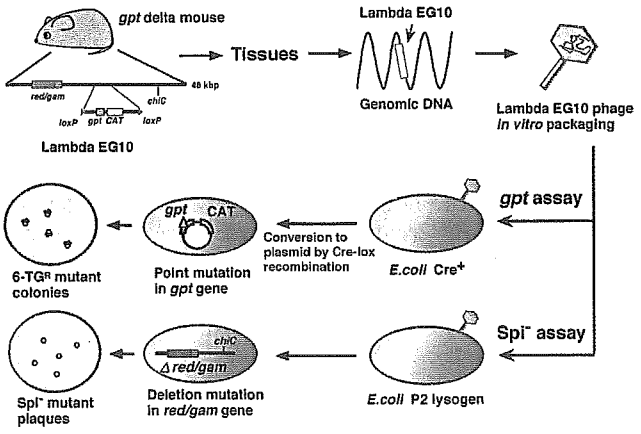

Figure 1 Scheme for *gpt* and Spi$^-$ assays for detecting mutations in gpt delta mice. The lambda EG10 phages are rescued from mouse genomic DNA by *in vitro* packaging. In *gpt* assay, lambda phages are infected into *E. coli* strain YG6020 expressing Cre recombinase and 6.4 kb region of lambda EG10, containing the *gpt* gene, was converted to plasmid. Mutation in *gpt* genes can be positively selected using a plate containing chloramphenicol and 6-TG. In Spi$^-$ assay, lambda phages are infected into *E. coli* harboring P2 lysogen. Lambda phages containing deletion mutations in *red/gam* genes can selectively grow and form Spi$^-$ mutant plaques

Results

Spontaneous mutations in the bone marrow of Parp-1$^{-/-}$ *mice*

In the *gpt* assay, which detects point mutations in the *gpt* gene (Figure 1), the spontaneous mutation frequencies of the bone marrow in *Parp-1*$^{+/+}$ and *Parp-1*$^{-/-}$ mice ($n=5$, respectively) were 6.9 ± 3.1 ($\times10^{-6}$), and 5.6 ± 1.2 ($\times10^{-6}$). There was no significant difference between *Parp-1*$^{+/+}$ and *Parp-1*$^{-/-}$ mice ($P=0.75$). The spectra and distribution patterns of the mutations in the *gpt* gene were not different between *Parp-1*$^{+/+}$ and *Parp-1*$^{-/-}$ mice (data not shown).

In the Spi$^-$ assay, which detects deletion mutations in the *red/gam* genes (Figure 1), mutant frequencies in *Parp-1*$^{-/-}$ and *Parp-1*$^{+/+}$ mice ($n=5$, respectively) were 8.0 ± 1.0 ($\times10^{-6}$) and 6.7 ± 2.0 ($\times10^{-6}$), respectively, and there was no significant difference between either genotype ($P=0.46$). The spectra and the distributions of the mutations in the *red/gam* genes were analysed with 39 and 27 mutants for *Parp-1*$^{-/-}$ and *Parp-1*$^{+/+}$ animals, respectively. Most of the mutations were deletion mutations of 1–6 bp at single-nucleotide run sequences and there was no difference in the distribution of mutation sites between the genotypes (data not shown).

Increase in Spi$^-$ mutant frequencies in the liver of BHP-treated Parp-1$^{-/-}$ *mice*

Genomic DNA was prepared from the liver, a major target organ of BHP (Green *et al.*, 1980). Mutant frequency of the *gpt* gene in the livers of nontreated mice ($n=4$) was 5.7 ± 0.9 ($\times10^{-6}$) and 10 ± 1.8 ($\times10^{-6}$) in *Parp-1*$^{+/+}$ and *Parp-1*$^{-/-}$ mice, respectively. After BHP treatment, mutant frequencies were increased to 89 ± 6.4 ($\times10^{-6}$) and 66 ± 12 ($\times10^{-6}$), respectively. There was no significant difference between the genotypes of the nontreated ($P=0.059$) and the BHP-treated mice ($P=0.083$) (see Supplementary Information).

Spi$^-$ mutant frequencies in nontreated *Parp-1*$^{+/+}$ and *Parp-1*$^{-/-}$ mice were not statistically different ($P=0.083$). On the other hand, Spi$^-$ mutant frequencies in BHP-treated mice increased to 16 ± 2.0 ($\times10^{-6}$) and 26 ± 4.2 ($\times10^{-6}$), respectively. The mutant frequency in *Parp-1*$^{-/-}$ mice was 1.6-fold higher compared with *Parp-1*$^{+/+}$ mice ($P<0.05$, Table 1).

Analysis of mutation spectrum

Mutation spectra of 83 and 179 Spi$^-$ mutant phages rescued from *Parp-1*$^{+/+}$ and *Parp-1*$^{-/-}$ mice, respectively, were analysed as shown in Table 2. Most of the Spi$^-$ mutations were deletions and the specific mutation frequencies of the total deletion mutations were 1.7-fold higher in *Parp-1*$^{-/-}$ than in *Parp-1*$^{+/+}$ mice, although the

Table 1 Mutant frequency of the *red/gam* genes in the livers of nontreated and BHP-treated mice

BHP	*Genotype*	*Mouse identification no.*	*Titer ($\times 10^6$)*	*No. of Spi⁻ mutant plaques*	*Mutant frequency ($\times 10^{-6}$)*	
						Mean±s.e.
Control	*Parp-1*$^{+/+}$	G27	3.03	20	6.6	7.5±1.0
		G28	1.29	7	5.4	
		G53	2.91	24	8.2	
		G89	1.94	19	9.8	
	Parp-1$^{-/-}$	G19	1.03	8	7.8	3.6±1.5
		G23	3.16	4	1.3	
		G29	3.46	5	1.4	
		G68	1.31	5	3.8	
2 g/kg body weight	*Parp-1*$^{+/+}$	G79	1.30	14	11	16±2.0
		G81	1.47	26	18	
		G82	1.31	26	20	
		G84	1.13	17	15	
	Parp-1$^{-/-}$	G80	1.97	39	20	26±4.2
		G83	1.86	70	38	
		G86	1.67	43	26	
		G92	1.35	27	20	

*Significant difference between *Parp-1*$^{+/+}$ and *Parp-1*$^{-/-}$ mice ($P=0.038$)

Table 2 Mutation types and their frequencies in *red/gam* genes after treatment with BHP

Mutation type	Parp-1$^{+/+}$		Parp-1$^{-/-}$		*Fold-increase by* Parp-1 *deficiency*	
	No. of mutants (%)	*Specific mutation frequency±s.e. ($\times 10^{-6}$)*	*No. of mutants (%)*	*Specific mutation frequency±s.e. ($\times 10^{-6}$)*	*Fold*	P-*value*
Deletion	69 (85)	13.1±2.1	154 (88)	22.1±4.2	1.7	0.082
1 bp	34 (42)	6.4±1.7	75 (43)	10.5±2.4	1.7	0.15
2 bp–1 kbp	19 (23)	3.7±0.96	33 (19)	5.0±1.2	1.3	0.47
> 1 kbp	16 (20)	3.0±0.44	46 (26)	6.6±1.3	2.2*	0.021
Base substitution	11 (14)	2.1±0.23	12 (7)	1.7±0.31	0.81	0.31
1–2 bp insertion	1 (1)	0.17±0.17	9 (5)	1.3±0.47	7.9	0.091
Total	81 (100)[a]		175 (100)[b,a]			

*Significant difference in the frequency of > 1 kbp deletion mutations between *Parp-1*$^{+/+}$ and *Parp-1*$^{-/-}$ mice ($P<0.05$). [a]Identical mutants derived from the same mouse were counted as one mutation. [b]One Spi⁻ mutant from *Parp-1*$^{-/-}$ mice did not contain any mutation in *red/gam* genes and was excluded from the table

difference was not statistically significant ($P=0.082$). The Spi⁻ mutants were classified into three classes based on the deletion sizes, namely deletions of single base, 2 bp–1 kbp, and > 1 kbp, and we calculated each specific mutation frequency. The mutation frequencies of deletions larger than 1 kbp in *Parp-1*$^{-/-}$ mice were 2.2-fold higher than in *Parp-1*$^{+/+}$ mice ($P<0.05$). We also noticed that the specific mutation frequencies of 1–2 bp insertions in the *red/gam* genes were also 7.9-fold more in *Parp-1*$^{-/-}$ than in *Parp-1*$^{+/+}$ mice (Table 2), although the difference was not statistically significant ($P=0.091$). Notably, most of these insertions (8/9) were observed in mononucleotide adenine (thymine) runs in *Parp-1*$^{-/-}$ mice (Table 3). These 1 bp insertion and base substitution mutations might not be detected as Spi⁻ mutants if other P2 lysogenic *Escherichia coli* strain, such as WL95 (P2), were used (Nohmi and Masumura, 2004). In all, 71 and 80% of the single base deletions were located at 2–6 bp runs in *Parp-1*$^{+/+}$ and *Parp-1*$^{-/-}$ mice, respectively, and the sites of single base deletions in the *gam* gene of *Parp-1*$^{-/-}$ mice exhibited a wider distribution pattern, as shown in Figure 2. The locations of the hot spots for the single base deletions were neither different between genotypes nor from those reported for spontaneous mutations in the liver (Masumura *et al*., 2002).

Classification of BHP-induced deletion mutations with two bases or more

There was no difference in the distribution pattern of deletion mutations with two bases or more between the genotypes (Figure 3). Deletions of two bases or more were further categorized into simple- or complex-type deletions, including deletions with small insertions of 1–5 bp, recombinations, and rearrangements, by analysis of their deletion region/junction sequences (Table 4). Although the majority of the deletions were simple deletions both in *Parp-1*$^{+/+}$ and *Parp-1*$^{-/-}$ mice, the

Table 3 Insertion mutation of single or two bases in the *red/gam* genes of BHP-treated mice

	Mutant identification no.	*Insertion mutation*	*Original sequence (5′–3′)*	*Mutated sequence (5′–3′)*	*Insertion position in the* gam *gene*
Parp-1$^{+/+}$	Ls4 G81-1-8	c	gct*c*aga	gct*cc*aga	157
Parp-1$^{-/-}$	Ls6 G92-1-2	t	gtc*ttg*ag	gtc*ttt*gag	149–150
	Ls6 G92-2-5	a	agc*aaaaaaa*tcc	agc*aaaaaaaa*tcc	295–300
	Ls13 G92-1-4	a	agc*aaaaaaa*tcc	agc*aaaaaaaa*tcc	295–300
	Ls4 G83-2-8	aa	agc*aaaaaaa*tcc	agc*aaaaaaaaa*tcc	295–300
	Ls13 G83-1-3	c	tgg*c*aga	tgg*cc*aga	350
	Ls4 G80-1-10	a	ttg*aaa*cca	ttg*aaaa*cca	374–376
	Ls4 G80-2-9	a	ttg*aaa*cca	ttg*aaaa*cca	374–376
	Ls4 G80-2-13	a	ttg*aaa*cca	ttg*aaaa*cca	374–376
	Ls4 G83-1-10	a	ctc*a*cca	ctc*aa*cca	386

Underlined italic letters represent the sites of mutations

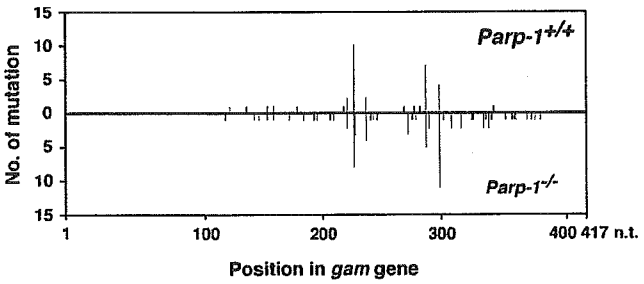

Figure 2 Distribution of single-base deletion mutations in the *gam* gene. Red bars indicate single-base deletions in a run of two to six bases of the same nucleotide; black bars indicate those not located in identical run sequences. Nucleotide 1 corresponds to the adenine residue in the first ATG of the *gam* gene. Total single base deletions show a wider distribution pattern in *Parp-1*$^{-/-}$ than in *Parp-1*$^{+/+}$ mice

ratio of complex-type deletions was significantly higher in *Parp-1*$^{-/-}$ compared to *Parp-1*$^{+/+}$ mice ($P<0.05$).

Mutants accompanying small insertions at the junction of deletions were observed in six of 73 (8.2%) in *Parp-1*$^{-/-}$ but none in *Parp-1*$^{+/+}$ mice (Table 4). Deletion mutants could be categorized into two types depending on the structures of the deletion junctions. If they harbor microhomology, they could possibly be produced during microhomology-mediated end joining (MEJ) and be classified as MEJ type (Figure 4) (Roth and Wilson, 1986). If the deletion junctions harbor no microhomology, they could possibly originate during non-microhomology-mediated end joining (non-MEJ) and could be classified as non-MEJ type (Figure 4). In non-MEJ, DNA termini are postulated to be processed to become blunt ended, and then both ends will be held together and ligation of DNA ends will be accomplished (Roth and Wilson, 1986).

Notably, five out of the six mutants from *Parp-1*$^{-/-}$ mice harbored no microhomology at deletion junctions, indicating that they were mostly caused by non-MEJ. Three mutants contained palindromic small insertions at deletion junctions (see the legend of Table 4).

Seven mutants from *Parp-1*$^{-/-}$ and two from *Parp-1*$^{+/+}$ mice (Table 4) were found to contain rearrangements (see Materials and methods for experiments). We also noticed that three mutants from *Parp-1*$^{-/-}$ mice accompanied recombinations, which occurred between the deleted regions of the *red/gam* genes and sequences in lambda EG10 (Table 5). As the lambda EG10 sequence is tandemly integrated in the genome, we could not determine whether these complex-type deletions were generated by reciprocal or nonreciprocal recombinations. Interestingly, two out of the three mutants harbored microhomology at the deletion junctions. On the other hand, the deletion in Ls4 G86-2-6 (Table 5) was suggested to occur through two sequential recombinations using 8–10 bp homologous sequences (underlined sequences in Table 5). Notably, 'Cttca' at junctional sequences of the deletion was common in two out of the three rearrangements (Table 5).

The fraction of deletion mutants that harbored short microhomology at the deletion junction, namely MEJ type to the total NHEJ event (the sum of MEJ-type and non-MEJ-type deletions), was 13/30 (43%) and 17/66 (26%) in *Parp-1*$^{+/+}$ and *Parp-1*$^{-/-}$ mice, respectively, showing a tendency for decrease of MEJ-type and increase of non-MEJ-type under *Parp-1* deficiency, although the difference is not statistically significant ($P=0.085$).

Discussion

The Spi$^-$ mutant frequencies were 1.6-fold higher in the liver of *Parp-1*$^{-/-}$ compared to *Parp-1*$^{+/+}$ mice after the treatment with BHP ($P<0.05$). Most of the mutations were found to be deletion types in both genotypes, and the specific mutation frequencies of deletion showed a 1.7-fold elevation in *Parp-1*$^{-/-}$ compared to *Parp-1*$^{+/+}$ cases, although the difference was not statistically significant ($P=0.082$). We further observed that *Parp-1* deficiency enhances deletion mutations, especially more than 1 kbp in size ($P<0.05$), and complex-type deletions accompanying either insertion or recombination/rearrangement in mice after treatment with BHP ($P<0.05$). On the other hand, the mutant frequencies in the *gpt* gene were elevated to the same level in both *Parp-1*$^{+/+}$ and *Parp-1*$^{-/-}$ mice, suggesting that *Parp-1*

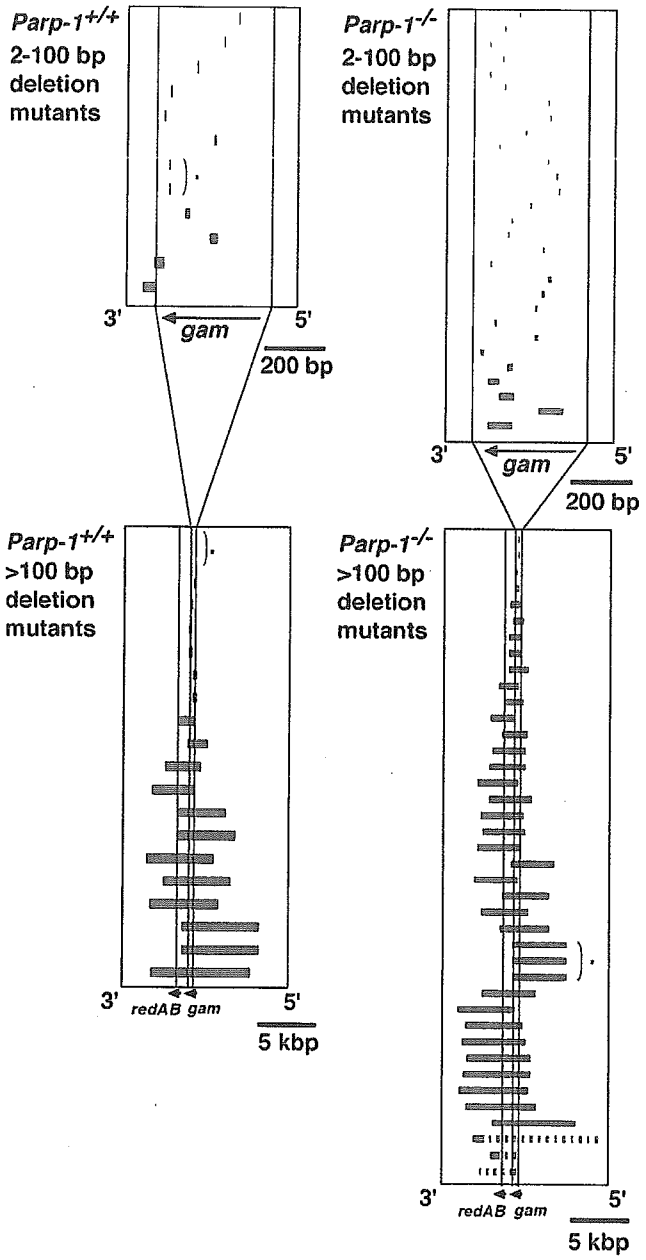

Figure 3 Distribution pattern of deletion mutations in the *red/gam* genes of the indicator bacteriophage. The two upper panels (**a, b**) show deletion of 2–100 bp. The two lower panels (**c, d**) show deletion of greater than 100 bp. The two left-hand panels (**a, c**) show the results in *Parp-1*$^{+/+}$, and the two right-hand panels (**b, d**) show the results in *Parp-1*$^{-/-}$ animals. Each red horizontal bar represents all observed deletions. The length of the bar indicates the size of the deletions. The horizontal axis shows the lengths of the genes that were used. The position of the bar shows the regions deleted in each example. The vertical axis has no significance. The individual observations are simply listed in measuring the sizes of the deletions. *Identical mutants from the same mouse

deficiency does not contribute substantially to the increase of point mutations even after treatment with the alkylating agent. The data suggested that *Parp-1* deficiency led to the enhancement of deletion mutation frequency after treatment with an alkylating agent, BHP, and this may directly relate to the higher incidence

Table 4 Classification of deletion mutations of two bases or more in the *red/gam* genes in BHP-treated mice

Deletion	No. of mutants					
	Parp-1$^{+/+}$			Parp-1$^{-/-}$		
	Total	*MEJ*	*Non-MEJ*	*Total*	*MEJ*	*Non-MEJ*
Simple	30	13	17	57	16	41
Complex-type						
With small insertion	0	0	0	6 *	1	5[a]
With recombination	0	0	0	3	0	3
With rearrangement	2	ND	ND	7	ND	ND
Total	32			73		

*Significant difference in complex-type deletion between *Parp-1*$^{+/+}$ and *Parp-1*$^{-/-}$ mice ($P = 0.047$). MEJ, microhomology-mediated end joining. Non-MEJ, nonmicrohomology-mediated end joining. ND, not determined. [a]Three mutants contained palindromic small insertions at deletion junction: 5′-GCCTCTTTCTCTTCA*a*TGCTGGTAGTGACGC-3′, 5′-GCTCATGTAATTTAT*ta*TAGTGAATGCTTTTG-3′, and 5′-CGGGCGAGCTGCTGG*cc*CGCGCCCAGCTCTGAGC-3′. Lowercase and underlined sequences indicate small insertions and palindromic sequences, respectively

of cancer development. Spontaneous mutant frequencies in bone marrow cells measured by both *gpt* and Spi$^-$ assays were not different between *Parp-1*$^{+/+}$ and *Parp-1*$^{-/-}$ animals at 4 months old ($P > 0.05$, respectively). This was expected since spontaneous tumor incidences, including those of lymphoma, were not elevated in *Parp-1*$^{-/-}$ mice at least until 9 months of age (Nozaki *et al.*, 2003), and the elevation of the incidence of hepatocellular carcinoma in *Parp-1*$^{-/-}$ mice was reported only at 18–24 months (Tong *et al.*, 2002). To understand the relationship of mutation and carcinogenesis, it will be helpful to measure mutant frequencies in *Parp-1*$^{+/+}$ and *Parp-1*$^{-/-}$ mice at advanced ages.

BHP mainly produces O^6- and N^7-methylguanines, and O^6- and N^7-hydroxypropylguanines as DNA lesions (Kokkinakis, 1992). O^6- and N^7-methylguanines can be repaired by BER or alkylguanine alkyltransferases, whereas O^6- and N^7-hydroxypropylguanines might be repaired not only by BER but also by nucleotide excision repair (Nivard *et al.*, 2003). Point mutations in the *gpt* gene after treatment with BHP are likely to be caused by translesion DNA synthesis through damaged bases. It was notable that the frequencies of 1–2 base adenine (thymine) insertions in the adenine (thymine) mononucleotide run sequences in *red/gam* genes showed a greater tendency in *Parp-1*$^{-/-}$ than in *Parp-1*$^{+/+}$ mice, although it was not statistically significant. These mutations could be caused by DNA polymerase slippage during replication. There is a possibility that either the frequencies of DNA polymerase slippage are higher or the subsequent mismatch repair is less efficient under *Parp-1* deficiency.

In the BER process, damaged bases are initially excised by DNA glycosylases, such as 8-oxoguanine-DNA glycosylase (OGG1) or endonuclease III homolog 1 (NTH1), and, subsequently, a single base gap is

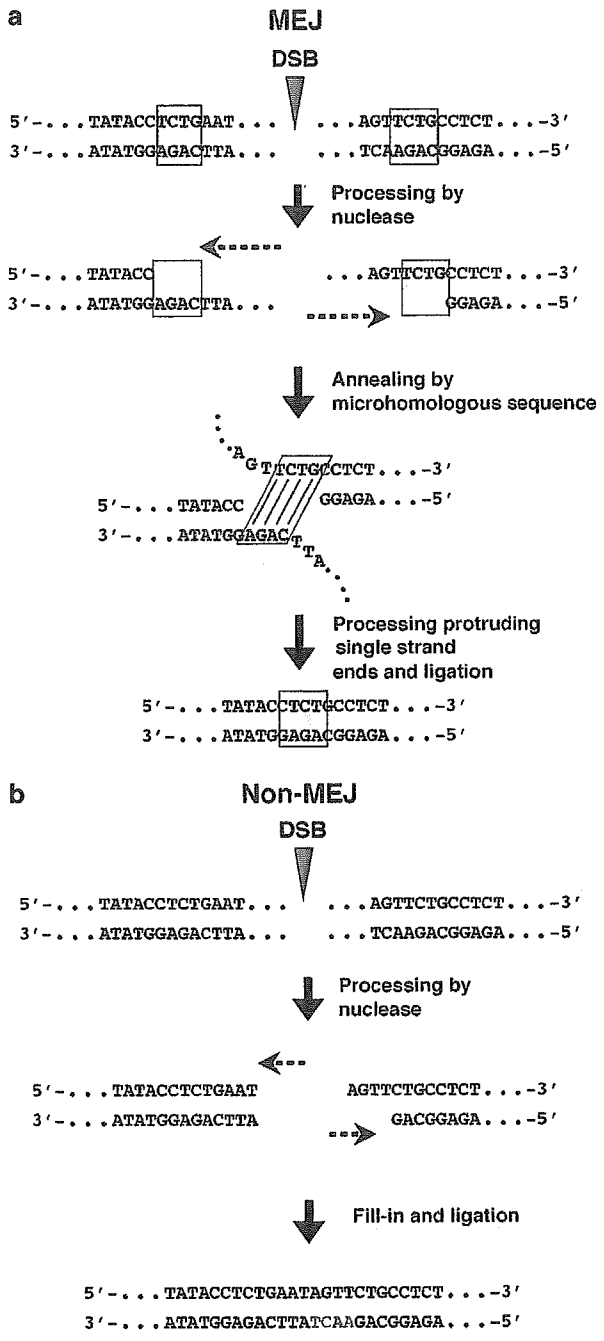

Figure 4 MEJ and non-MEJ reactions after introduction of DSB. (**a**) MEJ: After occurrence of DSB, both of the DNA termini are processed by nucleases, for example, Artemis, Mre11 or Werner syndrome protein (Paull and Gellert, 2000; Oshima *et al*., 2002; Lieber *et al*., 2003). When both ends reach a microhomologous sequence of 2–5 bases, excision of DNA is stopped and annealing occurs. After removing protruding single-stranded ends, ligation of both the strands occurs and the end-joining process is completed (Roth and Wilson, 1986). (**b**) Non-MEJ: Both DNA termini are either blunt ended when DSB occurred or processed to become blunt ended by nucleases. Then, both DNA ends may be held together by DNA-PKcs, Ku70/80, XRCC4 complex, and ligation of DNA ends will be carried out, probably by DNA ligase IV (Roth and Wilson, 1986)

generated by AP endonuclease activity, and nick sensor Parp-1 is recruited to DNA ends (Menissier-de Murcia *et al*., 1989). At later stages in BER, especially in the long-patch repair, Parp-1 facilitates DNA polymerization by interacting with polβ (Dantzer *et al*., 2000). Parp-1 also interacts with FEN-1, which excises approximately 2–7 base pairs to remove damaged bases in the long-patch repair (Prasad *et al*., 2001). The absence of difference in the mutant frequency of the *gpt* gene between *Parp-1*$^{-/-}$ and *Parp-1*$^{+/+}$ mice ($P>0.05$, see Supplementary Information) suggested that the BER pathway under *Parp-1* deficiency might possibly proceed until the excision of damaged bases.

The increase of deletion mutations accompanying insertion or recombination/rearrangement ($P<0.05$, see Table 4) indicated two possibilities, namely, DSB repair occurred more frequently or the repair fidelity of DSBs was lower under *Parp-1* deficiency. As for the former possibility, a possible explanation is that DNA polymerization or the displacement step of BER might be stalled in the absence of Parp-1 by the inefficient recruitment of repair proteins and DNA gaps may not be sealed efficiently and properly. The experiment with the *in vitro* reconstituted system showed that Parp-1 stimulates strand displacement and the removal process of long patch repair in the presence of FEN-1 (Prasad *et al*., 2001). It is generally postulated that the stalled, gapped DNA intermediates in BER could possibly develop into DSBs (Harrison *et al*., 1999; Vispe *et al*., 2003). The DSBs might also be induced at a higher frequency in the absence of Parp-1 after treatment of BHP by stalled replication forks caused by the damaged bases, leading to a collapse of the holiday structure. It is shown that, in *Parp-1*$^{-/-}$ cells, the repair of stalled replication forks is delayed (Yang *et al*., 2004). Another possibility for generation of DSB after BHP treatment is that, in order to remove massive alkylated bases, abortive mismatch repair (Branch *et al*., 1993) or base excision repair (Blaisdell and Wallace, 2001) might occur and excessive incision reactions on DNA may result in introduction of DSBs.

The second possibility, namely lower fidelity of DSB repair under *Parp-1* deficiency, could be explained as follows. DSBs could be repaired mostly by either NHEJ or HR (Valerie and Povirk, 2003), and, because we found no long homology in the junctional sequences of any of the analysed simple deletion mutants, we suggest that most of the deletion mutations might be generated during NHEJ repair. The major process of NHEJ is catalysed by DNA-PKcs and the Ku70/80 complex. In the presence of both DNA-PKcs and Parp-1, autophosphorylation of DNA-PKcs is stimulated by Parp-1 (Ariumi *et al*., 1999). Parp-1 might also protect DSB termini from nuclease attack because polyADP-ribosylation of Ku70/80 reduces exonuclease activity of WRN *in vitro* (Li *et al*., 2004) and contributes to efficient recruitment and activation of DNA–PK complexes. It is thus speculated that the recruitment of DNA-PKcs or its activity could not be controlled in the absence of Parp-1, resulting in low fidelity of NHEJ repair.

Table 5 Complex-type deletion mutations accompanying recombination observed in *Parp-1*$^{-/-}$ mice

Mutant identification no.	*Original sequences (I) in lambda EG10*	*Original sequences (II) in lambda EG10*	*Junctional sequence of mutation*
Ls4 G80-1-2	5′-...CGCCCGTTTTctggatgcgg-3′ 3′-...GCGGGCAAAAgacctacgcc-5′ * * 13754[a] 13763	↓ 5′-...GGTGATGTCTtcaagtggag-3′ 3′-...CCACTACAGAagttcacctc-5′ * * 20625 20634	5′-...GGTGATGTCTAAAACGGGCG...-3′ 3′-...CCACTACAGATTTTGCCCGC...-5′
Ls4 G86-2-6	5′-cccggtggtctgCCCTGG...GGCTGCaggtgcagagtgat-3′ 3′-gggccaccagacGGGACC...CCGACGtccacgtctcacta-5′ * * 14354 14381 5′-...GCGTGGTCTGagtgtgttac-3′ 3′-...CGCACCAGACtcacacaatg-5′ * * 18893 18902	↓ 5′-...CCTGCTCTGCCGCTtcacgcagtg-3′ 3′-...GGACGAGACGGCGAagtgcgtcac-5′ * * 22456 22465	5′-...CTCTGCCGCTGCAGCC...CCAGGGCAGACCACGC...-3′ 3′-...GAGACGGCGACGTCGG...GGTCCCGTCTGGTGCG...-5′
Ls13 G83-1-6	5′-...ATTATGGGCCgccacgacga-3′ 3′-...TAATACCCGGcggtgctgct-5′ * * 1992 2001	↓ 5′-gggtatcatgTAGCCGCTTA...-3′ 3′-cccatagtacATCGGCGAAT...-5′ * * 26359 26368	5′-...ATTATGGGCCTAGCCGCTTA...-3′ 3′-...TAATACCCGGATCGGCGAAT...-5′

Lowercase indicates deleted sequences, and homologous sequences at junctions are underlined. Red and blue letters represent rearranged sequences. The *red/gam* gene is located at nucleotide positions from 24 921 to 23 450 in the sense orientation. [a]Nucleotide positions (as indicated by asterisk) in lambda EG10. ↓, the position of the deletion junctions. The upper red line indicates 'Cttca' sequences at deletion junctions, which is common to Ls4 G80-1-2 and Ls4 G86-2-6.

NHEJ is further classified into MEJ and non-MEJ; the former harbors some microhomology at DSB termini, whereas the latter harbors no microhomology (Figure 4). To ask whether the deletion mutations observed in *Parp-1*$^{-/-}$ and *Parp-1*$^{+/+}$ mice were caused through MEJ or non-MEJ, we categorized the Spi$^-$ mutants and calculated the fraction of MEJ frequency to total NHEJ events. The fraction is decreased to approximately half that in *Parp-1*$^{-/-}$ (26%) compared with that in *Parp-1*$^{+/+}$ mice (43%). We also found that the frequency of complex-type deletions accompanying 1–5 bp insertions or recombination/rearrangement is substantially increased ($P<0.05$), namely, 16/73 (22%) of the mutants in *Parp-1*$^{-/-}$ compared to 2/32 (6%) of those in *Parp-1*$^{+/+}$ cases (Table 4). In most of these cases, the deletion junction did not harbor microhomology. These results suggest that DNA ends may be destabilized in the absence of Parp-1 and allow accidental insertion or recombination/rearrangement in non-MEJ processes. The introduction of small insertions in deletion junctions could be caused by polymerase λ (pol λ) and pol μ, which facilitate filling of a few bases gap in the NHEJ, and terminal deoxynucleotidyl transferase (TdT), which is also involved in the NHEJ event of V(D)J recombination (Garcia-Diaz *et al.*, 2002; Bebenek *et al.*, 2003). In the absence of Parp-1, these error-prone DNA polymerases might easily modify these DNA ends, resulting in small insertions, namely nontemplated nucleotides.

Three of six mutants with small insertions contained 'palindromic (P) nucleotides' at deletion junctions under *Parp-1* deficiency (Table 4). 'P nucleotides' are possibly introduced by self-complementary single-strand extensions during the DSB repair process of V(D)J recombination, and slightly longer 'P nucleotides' insertions at a higher frequency could be observed in the deletion mutations of SCID mice (Ding *et al.*, 2003). The present results suggested the possibility that 'P nucleotides' may be preferentially introduced during NHEJ repair under *Parp-1* deficiency, possibly through the destabilization of DNA ends.

A higher frequency (10/73) of deletion mutations accompanying recombination/rearrangement was observed in *Parp-1*$^{-/-}$ animals than in *Parp-1*$^{+/+}$ animals (2/32) as shown in Table 4, although it is not statistically significant ($P>0.05$). Ls4 G86-2-6 mutation in Table 5 was suggested to involve two sequential recombinations using 8–10 bp homology (underlined). There is a possibility that this mutation could be caused by the switchover of NHEJ to HR repair during processing of DSBs. The possible involvement of Parp-1 in the regulation of switching from NHEJ to HR should be further investigated, because the elevated frequency of HR including gene targeting (Semionov *et al.*, 2003) and SCEs (de Murcia *et al.*, 1997) was reported previously in the absence of Parp-1 or by Parp-1 inhibition.

We observed more deletion mutations ($P=0.082$), especially those more than 1 kbp ($P<0.05$), and complex-type deletions accompanying either insertion or recombination/rearrangement ($P<0.05$) in *Parp-1*$^{-/-}$ mice. We suggested that this indicates that Parp-1 prevents these types of genomic changes. *In vitro* studies showed that Parp-2 also facilitates BER by interacting with DNA repair proteins such as XRCC1 (Schreiber *et al.*, 2002); however, the present result suggests that the role of Parp-1 in preventing these types of mutations could not be fully compensated by Parp-2 or other molecules engaged in DNA repair. It is reported that interstitial deletions in human cancer could be preferentially produced through NHEJ repair processes (Sasaki *et al.*, 2003), suggesting the substantial contribution of deletion mutation to carcinogenesis. Although the increase of Spi$^-$ mutant frequency by *Parp-1* deficiency is only 1.6-fold ($P<0.05$), this difference may evoke a significant impact on multi-step carcinogenesis (Doll, 1962; Sugimura, 1992). For example, if mutation in five genes is necessary for cancer development, the difference in the frequency of achieving all the five mutations between *Parp-1*$^{+/+}$ and *Parp-1*$^{-/-}$ mice is calculated to be 10-fold. The impact of *Parp-1* deficiency on deletion mutation might be different among tissues and DNA-damaging insults; however, the present results suggest a substantial role of Parp-1 in the maintenance of genomic stability, which may be important not only for carcinogenesis but also for various pathogenic processes. The results also raise a caution on the therapeutic use of Parp-1 inhibitors, and basic studies should be carried out carefully to avoid any possible risks to causing somatic or germ-cell mutations by Parp-1 inhibition.

Materials and methods

Establishment of Parp-1$^{-/-}$/gpt *delta mice*

Homozygous *gpt* delta transgenic mice of C57BL/6 genetic background (Nohmi *et al.*, 1996) were mated with *Parp-1*$^{-/-}$ mice of ICR/129Sv mixed genetic background (Masutani *et al.*, 1999), and *Parp-1*$^{+/-}$ mice homozygous for the lambda EG10 transgene (*Parp-1*$^{+/-}$*/gpt* delta mice) were obtained. By intercrossing *Parp-1*$^{+/-}$*/gpt* delta mice, we obtained *Parp-1*$^{-/-}$*/gpt* delta and *Parp-1*$^{+/+}$*/gpt* delta animals.

Animal treatment

Spontaneous mutant frequencies in the bone marrow and livers were analysed as follows. Male *Parp-1*$^{+/+}$ and *Parp-1*$^{-/-}$ mice ($n=5$, respectively) were fed a basal diet (CE-2, Clea Japan), anesthetized, and killed at the age of 16 weeks. The bone marrows and livers were immediately frozen in liquid nitrogen, and stored at −80°C until DNA extraction.

BHP (Nakalai Tesque) was dissolved in saline, adjusted to 0.2 g/ml, and sterilized by filtration. Four *Parp-1*$^{-/-}$*/gpt* delta and four *Parp-1*$^{+/+}$*/gpt* delta male mice received an intraperitoneal injection of BHP at 2 g/kg body weight (bw) at the age of 16 weeks. All animals were killed 1 week after BHP administration, and the livers were frozen and stored as described above. Genomic DNAs were extracted from the bone marrows and livers by standard phenol/chloroform extraction or the dialysis method performed with a Recover-Ease DNA isolation kit (Stratagene). A lambda phage *in vitro* packaging reaction was carried out with Transpack Packaging Extract (Stratagene). The experimental protocol was approved

by the Ethics Review Committees for Animal Experimentation of the participating institutions.

gpt *assay*

The *gpt* assay (Figure 1) was performed as described previously (Nohmi *et al.*, 1996). Briefly, the phages rescued from genomic DNAs were transfected into *E. coli* YG6020 expressing Cre recombinase. Infected cells were cultured at 37°C on plates containing chloramphenicol (Cm) and 6-thioguanine (6-TG) for 3 days until 6-TG-resistant colonies appeared. To confirm the 6-TG-resistant phenotype, colonies were restreaked on plates containing Cm and 6-TG. Confirmed 6-TG-resistant colonies were cultured, and bacterial pellets were collected by centrifugation. The average background mutant frequency in the *gpt* assay was 1×10^{-6}. The predominant type of the background mutations is insertion of transposable element, IS*1* of *E. coli*, and is distinguishable from the mutations generated in mice (Masumura *et al.*, 1999). As no IS*1* insertion mutations were observed in our collection of *gpt* mutations recovered from mice, they were suggested to be originated in mice but not in *E. coli* host. The data for mutant frequencies in *gpt* assay were therefore presented without subtracting the average background mutant frequencies.

A 739 bp DNA fragment encompassing the *gpt* gene was amplified by PCR as described previously (Masumura *et al.*, 1999). DNA sequencing of the *gpt* gene was performed with a CEQ™ DTCS Quick Start Kit (Beckman Coulter).

Spi⁻ assay

An Spi⁻ assay (sensitive to P2 interference) (Nohmi *et al.*, 1996) was carried out with a slight modification as described previously (Shibata *et al.*, 2003). The frequencies of background mutants were less than 10^{-8} in Spi⁻ assay (Nohmi *et al.*, 1999) and was neglectable. The data for Spi⁻ mutant frequencies were therefore presented without subtracting the background mutant frequencies. Spi⁻ mutant phages were infected to *E. coli* LE392 and phage DNA was purified by Quantum Prep® AquaPure Genomic DNA Kit (Bio-Rad).

Analysis of mutation spectra in the Spi⁻ mutants

To determine the mutated region, lysates of Spi⁻ mutant phage or the phage DNA were used and subjected to PCR analysis with various sets of primers (Nohmi *et al.*, 1999; Okada *et al.*, 1999). To narrow down the mutated region, the structure of each mutation was also analysed by digesting Spi⁻ mutant DNA with restriction enzymes and by comparing the lengths of the produced fragments with those expected for wild-type lambda EG10 DNA. We also adapted a Southern blot hybridization method that uses oligonucleotide DNA probes (Shibata *et al.*, 2004). Briefly, 10 μg of oligomers, 25–36 nucleotides long, were spotted onto Hybond™-N (Amersham Pharmacia Biotech), and after crosslinking by UV (1200 J/m², Stratagene) the membrane was soaked into a hybridization buffer consisting of 10 × Denhardt's solution, 2 × SSC, and 100 μg/ml denatured salmon sperm DNA at 42°C for 2 h. As the probe of each clone, the 15 kb region spanning the *red/gam* genes of each Spi⁻ mutant was amplified by PCR with the primers 18874R and 32890F (Shibata *et al.*, 2004), and was labeled with [α-^{32}P]dCTP using the Megaprime DNA Labeling System (Amersham Pharmacia Biotech). Hybridization was performed overnight at 37°C, and the membrane was washed three times each for 1 h at 37°C with a buffer containing 2 × SSC, 0.1% SDS, and 7.5 mM pyrophosphate, and the radioactivity of each oligomer spot was analysed by BAS 2500 (Fuji Film). This method permits the identification of where a deletion occurred and its approximate length. When there is a deletion associated with an insertion, then one or more of the probes does not give a signal, but the PCR product is bigger than expected.

Statistical analysis

The statistical significance of differences in mutant or mutation frequencies between the two groups was analysed using the Mann–Whitney *U*-test. The differences of the frequencies of simple deletion and complex-type deletion between genotypes were analysed by Fisher's exact test.

Acknowledgements
We appreciate the help and suggestions provided by M Tsutsumi in histopathological examinations and suggestions, and thank K Nakamoto, T Nozaki, and H Fujihara for technical assistance. We are grateful to M Yanagihara for maintenance of the animals. This work was supported in part by a Grant-in-Aid for the Second Term Comprehensive 10-Year Strategy for Cancer Control, and a Grant-in-Aid for Scientific Research on Priority Areas from the Ministry of Education, Science, Sports, and Culture of Japan (15025274).

References

Adolph KW and Song MK. (1985). *Biochemistry*, **24**, 345–352.
Ariumi Y, Masutani M, Copeland TD, Mimori T, Sugimura T, Shimotohno K, Ueda K, Hatanaka M and Noda M. (1999). *Oncogene*, **18**, 4616–4625.
Bebenek K, Garcia-Diaz M, Blanco L and Kunkel TA. (2003). *J. Biol. Chem.*, **278**, 34685–34690.
Blaisdell JO and Wallace SS. (2001). *Proc. Natl. Acad. Sci. USA*, **98**, 7426–7430.
Branch P, Aquilina G, Bignami M and Karran P. (1993). *Nature*, **362**, 652–654.
Buki KG, Bauer PI, Hakam A and Kun E. (1995). *J. Biol. Chem.*, **270**, 3370–3377.
Caldecott KW, Aoufouchi S, Johnson P and Shall S. (1996a). *Nucleic Acids Res.*, **24**, 4387–4394.
Caldecott KW, Aoufouchi S, Johnson P and Shall S. (1996b). *Nucleic Acids Res.*, **24**, 4387–4394.
Dantzer F, de La Rubia G, Menissier-De Murcia J, Hostomsky Z, de Murcia G and Schreiber V. (2000). *Biochemistry*, **39**, 7559–7569.
de Murcia JM, Niedergang C, Trucco C, Ricoul M, Dutrillaux B, Mark M, Oliver FJ, Masson M, Dierich A, LeMeur M, Walztinger C, Chambon P and de Murcia G. (1997). *Proc. Natl. Acad. Sci. USA*, **94**, 7303–7307.
Ding Q, Reddy YV, Wang W, Woods T, Douglas P, Ramsden DA, Lees-Miller SP and Meek K. (2003). *Mol. Cell. Biol.*, **23**, 5836–5848.
Doll R. (1962). *Gerontol. Clin. (Basel)*, **4**, 211–221.
El-Khamisy SF, Masutani M, Suzuki H and Caldecott KW. (2003). *Nucleic Acids Res.*, **31**, 5526–5533.
Galande S and Kohwi-Shigematsu T. (1999). *J. Biol. Chem.*, **274**, 20521–20528.
Garcia-Diaz M, Bebenek K, Sabariegos R, Dominguez O, Rodriguez J, Kirchhoff T, Garcia-Palomero E, Picher AJ,

Juarez R, Ruiz JF, Kunkel TA and Blanco L. (2002). *J. Biol. Chem.*, **277,** 13184–13191.
Green U, Konishi Y, Ketkar MB and Althoff J. (1980). *Cancer Lett.*, **9,** 257–261.
Harrison L, Hatahet Z and Wallace SS. (1999). *J. Mol. Biol.*, **290,** 667–684.
Kokkinakis DM. (1992). *Carcinogenesis*, **13,** 759–765.
Leppard JB, Dong Z, Mackey ZB and Tomkinson AE. (2003). *Mol. Cell. Biol.*, **23,** 5919–5927.
Li B, Navarro S, Kasahara N and Comai L. (2004). *J. Biol. Chem.*, **279,** 13659–13667.
Lieber MR, Ma Y, Pannicke U and Schwarz K. (2003). *Nat. Rev. Mol. Cell Biol.*, **4,** 712–720.
Masson M, Niedergang C, Schreiber V, Muller S, Menissier-de Murcia J and de Murcia G. (1998). *Mol. Cell. Biol.*, **18,** 3563–3571.
Masumura K, Kuniya K, Kurobe T, Fukuoka M, Yatagai F and Nohmi T. (2002). *Environ. Mol. Mutagen.*, **40,** 207–215.
Masumura K, Matsui M, Katoh M, Horiya N, Ueda O, Tanabe H, Yamada M, Suzuki H, Sofuni T and Nohmi T. (1999). *Environ. Mol. Mutagen.*, **34,** 1–8.
Masutani M, Nozaki T, Nakamoto K, Nakagama H, Suzuki H, Kusuoka O, Tsutsumi M and Sugimura T. (2000). *Mutat. Res.*, **462,** 159–166.
Masutani M, Suzuki H, Kamada N, Watanabe M, Ueda O, Nozaki T, Jishage K, Watanabe T, Sugimoto T, Nakagama H, Ochiya T and Sugimura T. (1999). *Proc. Natl. Acad. Sci. USA*, **96,** 2301–2304.
Menissier-de Murcia J, Molinete M, Gradwohl G, Simonin F and de Murcia G. (1989). *J. Mol. Biol.*, **210,** 229–233.
Morrison C, Smith GC, Stingl L, Jackson SP, Wagner EF and Wang ZQ. (1997). *Nat. Genet.*, **17,** 479–482.
Nivard MJ, Czene K, Segerback D and Vogel EW. (2003). *Mutat. Res.*, **529,** 95–107.
Nohmi T, Katoh M, Suzuki H, Matsui M, Yamada M, Watanabe M, Suzuki M, Horiya N, Ueda O, Shibuya T, Ikeda H and Sofuni T. (1996). *Environ. Mol. Mutagen.*, **28,** 465–470.
Nohmi T and Masumura K. (2004). *Adv. Biophys.*, **38,** 97–121.
Nohmi T, Suzuki M, Masumura K, Yamada M, Matsui K, Ueda O, Suzuki H, Katoh M, Ikeda H and Sofuni T. (1999). *Environ. Mol. Mutagen.*, **34,** 9–15.
Nozaki T, Fujihara H, Watanabe M, Tsutsumi M, Nakamoto K, Kusuoka O, Kamada N, Suzuki H, Nakagama H, Sugimura T and Masutani M. (2003). *Cancer Sci.*, **94,** 497–500.
Oikawa A, Tohda H, Kanai M, Miwa M and Sugimura T. (1980). *Biochem. Biophys. Res. Commun.*, **97,** 1311–1316.
Okada N, Masumura K, Nohmi T and Yajima N. (1999). *Environ. Mol. Mutagen.*, **34,** 106–111.
Okano S, Lan L, Caldecott KW, Mori T and Yasui A. (2003). *Mol. Cell. Biol.*, **23,** 3974–3981.
Oshima J, Huang S, Pae C, Campisi J and Schiestl RH. (2002). *Cancer Res.*, **62,** 547–551.
Paull TT and Gellert M. (2000). *Proc. Natl. Acad. Sci. USA*, **97,** 6409–6414.
Prasad R, Lavrik OI, Kim SJ, Kedar P, Yang XP, Vande Berg BJ and Wilson SH. (2001). *J. Biol. Chem.*, **276,** 32411–32414.
Roth DB and Wilson JH. (1986). *Mol. Cell. Biol.*, **6,** 4295–4304.
Sanderson RJ and Lindahl T. (2002). *DNA Repair (Amst.)*, **1,** 547–558.
Sasaki S, Kitagawa Y, Sekido Y, Minna JD, Kuwano H, Yokota J and Kohno T. (2003). *Oncogene*, **22,** 3792–3798.
Schreiber V, Ame JC, Dolle P, Schultz I, Rinaldi B, Fraulob V, Menissier-de Murcia J and de Murcia G. (2002). *J. Biol. Chem.*, **277,** 23028–23036.
Semionov A, Cournoyer D and Chow TY. (1999). *Nucleic Acids Res.*, **27,** 4526–4531.
Semionov A, Cournoyer D and Chow TY. (2003). *Biochem. Cell Biol.*, **81,** 17–24.
Shibata A, Masutani M, Kamada N, Masumura KI, Nakagama H, Kobayashi S, Teraoka H, Suzuki H and Nohmi T. (2004). *Environ. Mol. Mutagen.*, **43,** 204–207.
Shibata A, Masutani M, Nozaki T, Kamada N, Fujihara H, Masumura K, Nakagama H, Sugimura T, Kobayashi S, Suzuki H and Nohmi T. (2003). *Environ. Mol. Mutagen.*, **41,** 370–372.
Sugimura T. (1992). *Science*, **258,** 603–607.
Susse S, Scholz CJ, Burkle A and Wiesmuller L. (2004). *Nucleic Acids Res.*, **32,** 669–680.
Tong WM, Cortes U, Hande MP, Ohgaki H, Cavalli LR, Lansdorp PM, Haddad BR and Wang ZQ. (2002). *Cancer Res.*, **62,** 6990–6996.
Tsutsumi M, Masutani M, Nozaki T, Kusuoka O, Tsujiuchi T, Nakagama H, Suzuki H, Konishi Y and Sugimura T. (2001). *Carcinogenesis*, **22,** 1–3.
Valerie K and Povirk LF. (2003). *Oncogene*, **22,** 5792–5812.
Vispe S, Ho EL, Yung TM and Satoh MS. (2003). *J. Biol. Chem.*, **278,** 35279–35285.
Vodenicharov MD, Sallmann FR, Satoh MS and Poirier GG. (2000). *Nucleic Acids Res.*, **28,** 3887–3896.
Waldman BC and Waldman AS. (1990). *Nucleic Acids Res.*, **18,** 5981–5988.
Wang ZQ, Stingl L, Morrison C, Jantsch M, Los M, Schulze-Osthoff K and Wagner EF. (1997). *Genes Dev.*, **11,** 2347–2358.
Wesierska-Gadek J, Schmid G and Cerni C. (1996). *Biochem. Biophys. Res. Commun.*, **224,** 96–102.
Yang YG, Cortes U, Patnaik S, Jasin M and Wang ZQ. (2004). *Oncogene*, **23,** 3872–3882.
Yoshihara K, Hashida T, Yoshihara H, Tanaka Y and Ohgushi H. (1977). *Biochem. Biophys. Res. Commun.*, **78,** 1281–1288.

Supplementary Information accompanies the paper on Oncogene website (http://www.nature.com/onc)

Up-regulation of *hnRNP A1* gene in sporadic human colorectal cancers

MITSUNORI USHIGOME[1,2], TSUNEYUKI UBAGAI[1], HIROKAZU FUKUDA[1], NAOTO TSUCHIYA[1], TAKASHI SUGIMURA[1], JUN TAKATSUKA[2] and HITOSHI NAKAGAMA[1]

[1]Biochemistry Division, National Cancer Center Research Institute, 5-1-1 Tsukiji, Chuo-ku, Tokyo 104-0045; [2]Second Department of Surgery, Toho University School of Medicine, 6-11-1 Omori-nishi, Ota-ku, Tokyo 143-8541, Japan

Received August 12, 2004; Accepted November 2, 2004

Abstract. We have previously reported that the heterogeneous nuclear ribonucleoprotein A1 (hnRNP A1), a major hnRNP, binds to G-rich repetitive sequences and quadruplex (G4') structures in DNA, including the 5'-TTAGGG-3' telomere repeat and 5'-GGCAG-3' short-tandem-repeat. DNA synthesis arrest at the (GGG) sites within these repeats *in vitro* was retrieved by the addition of the hnRNP A1 protein or its N-terminal proteolytic product, UP1, in a dose-dependent manner. Therefore, functional perturbation of hnRNP A1 may abrogate the genomic stability of telomere repeats and other G-rich sequences, independent of its major role in transcriptional and translational regulation. In the present study, we conducted genetic and expression analysis of the *hnRNP A1* gene in sporadic human colorectal cancers to clarify its possible involvement in human carcinogenesis. Of 30 lesions, one harbored a mutation at the -11 position from the translation initiation site, but none in the coding region. A single nucleotide polymorphism, an A or G-allele, was found in the 5' upstream promoter region of the gene. Quantitative gene expression analysis revealed that 60% (18/30) of cases showed over-expression of *hnRNP A1* in cancer tissues by 2-fold or greater, compared to their normal colon tussues, with values of 78, 64 and 40% for clinicopathological stages II, III and IV, respectively. Although the biological consequences of *hnRNP A1* overexpression in colorectal cancers remain to be clarified, it could contribute to maintenance of telomere repeats in cancer cells with enhanced cell proliferation. Alternatively, since the variations in the stoichiometry of hnRNP family proteins are considered to affect cell-specific gene expression, quantitative alteration of hnRNP A1 could result in facilitation of transformation of colon epithelial cells as a consequence of transcriptional and translational perturbation.

Correspondence to: Dr Hitoshi Nakagama, Biochemistry Division, National Cancer Center Research Institute, 5-1-1 Tsukiji, Chuo-ku, Tokyo 104-0045, Japan
E-mail: hnakagam@gan2.res.ncc.go.jp

Abbreviations: hnRNP A1, heterogeneous nuclear ribonucleoprotein A1; RT-PCR, reverse transcribed-polymerase chain reaction; SSCP, single strand conformation polymorphism

Key words: hnRNP A1, colorectal cancer, RT-PCR, promoter, SNP

Introduction

Cancers develop after accumulation of multiple genetic and epigenetic alterations (1,2), and current progress in genome-wide comprehensive gene expression analysis has revealed that hundreds of genes are differentially expressed in colorectal cancer tissues compared to their normal counterparts (3,4). Molecular events at the translational level, due to epigenetic mechanisms, have recently been suggested to have a substantial impact on cancer development (5-7). Heterogeneous nuclear ribonucleoproteins (hnRNPs) are known as pre-mRNA/mRNA binding proteins and involved in various nuclear and cytoplasmic processes (8), such as biogenesis, splicing and nucleo-cytoplasmic transport of mRNA, and transcriptional and translational regulation (9-15). Furthermore, relative amounts of hnRNP family proteins can affect alternative splicing patterns (16,17) and the variations in stoichiometry of hnRNPs could also affect cell-specific gene expression (18). Therefore, quantitative and qualitative alterations of hnRNP family proteins may disturb both transcription and translation in cells, and facilitate malignant transformation (19).

To date, at least 20 major hnRNP proteins, from hnRNP A1 to U, have been identified in human cells (20). We have demonstrated that the hnRNP A1 protein, one of the major members of the hnRNP family, binds to quadruplex structures formed in G-rich repetitive DNA sequences, including the 5'-TTAGGG-3' telomere repeat and 5'-GGCAG-3' short-tandem-repeat (STR) (21,22). hnRNP A1 and UP1, an amino-terminal proteolytic product of hnRNP A1, have been shown to unwind the intramolecular folded-back quadruplex (G4') structures of telomere repeats and G-rich STRs as mentioned above, and abrogate DNA synthesis arrest at (GGG) sites within these repeats (23). It is interesting to note in this context that hnRNP A1-deficient mouse embryonic fibroblasts (MEFs) manifest decrease in telomere repeat length (24,25). Taking the available results together, functional alteration of the hnRNP A1 (or UP1) protein, either quantitatively or qualitatively, could be responsible for genomic instability at

Table I. List of primer sets used for PCR-SSCR and real-time RT-PCR analyses.

Gene	Primer set	Amplified region	Forward primer	Reverse primer	Tm (°C)	Product size
hnRNP A1	PR-1	Promoter region 1	5'-gataagactgtctgccactacc-3'	5'-gttgaccgcacgtgtagta-3'	60	352
	PR-2	Promoter region 2	5'-ctcagaggcaggtggaactt-3'	5'-gctttcggcattggtagact-3'	57	417
	E1	Exon 1	5'-atccaatcagagctgttcca-3'	5'-gcagcatcttaccgattcag-3'	57	250
	E2	Exon 2	5'-cgtgttgtagcccatttaacac-3'	5'-agcattcggagaagactgca-3'	60	236
	E3	Exon 3	5'-cttttgcggtcagactttgtg-3'	5'-tccatagcagcacatatccaag-3'	60	251
	E4	Exon 4	5'-tcgagtataggctttgctaatc-3'	5'-tgccatacagattgtggaac-3'	54	309
	E5-6	Exons 5 and 6	5'-ccctgataccatgttgtatct-3'	5'-agatggtgagaagtcagaact-3'	53	352
	E7	Exon 7	5'-gaactgcattcagaatgtcact-3'	5'-tcacagcatgcgtgttatg-3'	57	263
	E8	Exon 8	5'-cataacacgcatgctgtgag-3'	5'-cagtgtaccacacaatgcttc-3'	57	351
	E9	Exon 9	5'-aacatcatcctcaggtaacag-3'	5'-cagcagtagctacagacactc-3'	54	259
	E10	Exon 10	5'-cattactgttggcactttga-3'	5'-gttattgggttcatcagcaa-3'	54	170
hnRNP A1	A1-E3/E4	cDNA fragment encompassing exons 3, 4	5'-gtcacaatgccac-tgtggag-3'	5'-ggtcagtcatgatttcaatcac-3'	60	241
ß-actin	ßAc-E3	cDNA fragment in exon 4	5'-gacttcgagcaagagatggc-3'	5'-aggaaggaaggctggaagag-3'	58	137

G-rich repeats and/or G4' structures in the genome and thus be implicated in cell transformation and consequently cancer development.

In the present study, we analyzed genetic and epigenetic alterations of the *hnRNP A1* gene in sporadic human colorectal cancers, and found up-regulation in more than half of the cases. However, genetic alterations, including single nucleotide polymorphisms (SNPs), were demonstrated to be rare within the coding region of the *hnRNP A1* gene.

Materials and methods

Patients and tissue specimens. Paired surgical specimens of primary colorectal cancers and surrounding non-cancerous counterparts of the colon were obtained from 30 patients treated at the National Cancer Center Hospital, Tokyo, Japan, with documented informed-consent in each case. Samples were frozen in liquid nitrogen and stored at -80°C until use. The patients comprised 23 males and 7 females, the average ages being 65.0±9.5 (ranging from 45 to 83) and 63.4±11.1 (ranging from 41 to 73), respectively. All cases were diagnosed as sporadic colorectal cancers on the basis of absence of familial accumulation of cancer patients. Clinicopathological staging of cancers was accomplished according to the criteria approved by the American Joint Committee on Cancer (26). Histological diagnosis was performed following the WHO International Histological Classification of Tumors (27). Nine cases were stage II without lymph node metastasis, 11 cases were stage III with lymph node metastasis and 10 cases were stage IV with lymph node metastasis.

Mutation analysis of the hnRNP A1 gene. Genomic DNA was extracted and purified according to the standard phenol/chloroform procedure from approximately 50 mg samples of cancer and surrounding normal tissues. An aliquot of 50 ng genomic DNA was amplified by polymerase chain reaction (PCR) using 9 primer sets, which were designed from intron sequences to amplify all ten coding exons, and 2 primer sets amplifying an approximately 0.7 kbp 5'-promoter region of the *hnRNP A1* gene. One primer set, E5-6, was designed to amplify the genomic fragment encompassing exons 5 and 6. Nucleotide sequences of all primers and their annealing temperatures are listed in Table I. PCR amplification was performed in a total of 6 µl of reaction buffer, containing 50 ng of genomic DNA, 2.8 pmoles of each primer, 0.25 µM of dNTPs, 25.6 µCi of [α-^{32}P]dCTP (Amersham Pharmacia Biotech, NJ, USA), 0.6 µl of 10X PCR buffer (*TaKaRa* 10X PCR buffer) and 0.06 µl of *TaKaRa Ex Taq*™ (5 U/µl). The cycling program for each primer pair was set as follows, 94°C for 1 min followed by 30-35 cycles of 94°C for 30 sec, annealing temperature (53-60°C) for 30 sec, 72°C for 45 sec, followed by 72°C for 7 min. ^{32}P-labeled PCR products were subjected to PCR-single strand conformation polymorphism (PCR-SSCP) analysis according to a standard protocol (28). When shifted bands were detected, bands were eluted from the gel and re-amplified using the same primer sets, and subjected to PCR-based direct sequencing on an ABI Prism 310 Genetic Analyzer using a BigDye Terminator Cycle Sequencing Ready Reaction Kit (Amersham Pharmacia Biotech).

Quantitative RT-PCR analysis for hnRNP A1. Total RNA was isolated from approximately 30 µg frozen samples using Isogen (Nippon Gene, Japan) according to the manufacturer's instructions. After treatment with DNase I (TaKaRa Biomedicals, Japan), 2 µg aliquots were used for cDNA synthesis using the Superscript™ First-Strand Synthesis System (Invitrogen, CA, USA) with Oligo(dT)$_{12-18}$ primers. Primer sequences used to amplify the *hnRNP A1*

Table II. Clinicopathological features of human colorectal cancers and hnRNP A1 expression levels.

Case	Location[a]	Sex	Age (yr)	Histology[b]	Stage	SNP genotype[c]	hnRNPA1 mRNA copy no./ß-actin mRNA copy no.[d]		
							Normal (N)	Cancer (T)	T/N ratio
1	S	M	63	W	II	AG	0.31	1.90	6.1
2	R	F	58	M	II	GG	0.074	0.42	5.7
3	S	M	83	M	II	AA	0.17	0.85	5.0
4	R	M	61	M	II	AA	0.12	0.47	3.9
5	As	F	71	M	II	AA	0.12	0.31	2.6
6	R	M	51	M	II	AG	0.14	0.34	2.4
7	R	M	57	W	II	AG	0.71	1.54	2.2
8	R	M	63	M	II	GG	0.56	0.53	0.95
9	R	M	65	M	II	GG	0.88	0.05	0.057
10	S	M	67	W	III	AG	0.042	1.24	29.5
11	R	F	64	M	III	AG	0.16	1.32	8.3
12	R	M	64	M	III	GG	0.20	1.20	6.0
13	R	M	72	Por	III	AA	0.26	0.83	3.2
14	R	F	73	Mu	III	AA	0.23	0.61	2.7
15	R	M	81	Mu	III	AA	0.25	0.62	2.5
16	Ce	M	61	M	III	GG	0.53	1.15	2.2
17	Ce	F	66	W	III	AA	0.078	0.15	1.9
18	R	M	73	M	III	AA	0.18	0.30	1.7
19	R	M	61	M	III	GG	0.13	0.19	1.5
20	R	M	70	W	III	GG	0.11	0.087	0.79
21	S	M	72	M	IV	AA	0.49	2.30	4.7
22	R	M	69	M	IV	AG	0.14	0.62	4.4
23	De	M	59	W	IV	AG	0.17	0.60	3.5
24	Ce	F	41	W	IV	AG	0.30	0.63	2.1
25	T	M	45	M	IV	AG	0.26	0.44	1.7
26	R	F	71	M	IV	AG	0.24	0.38	1.6
27	S	M	55	Mu	IV	AG	0.35	0.45	1.3
28	S	M	78	W	IV	AA	0.19	0.23	1.2
29	S	M	53	M	IV	GG	0.16	0.14	0.88
30	S	M	71	M	IV	AG	0.53	0.39	0.74
Avr±SD							0.27±0.20	0.68±0.55	3.71±5.24

[a]Ce, cecum; As, ascending colon; T, transverse colon; De, descending colon; S, sigmoid colon; R, rectum. [b]W, well-differentiated; M, moderately-differentiated; Por, poorly-differentiated; Mu, mucinous. [c]AA, homozygous for adenine (A)-allele; GG, homozygous for guanine (G)-allele; AG, heterozygous for A- and G-alleles in the 5'-promoter region. [d]Copy numbers of the transcripts were evaluated using standard curves generated with the known copy numbers of plasmid containing hnRNPA1 and ß-actin cDNA fragments, respectively, as detailed in Materials and methods.

cDNA were 5'-GTCACAATGCCACTGTGGAG-3' (forward) and 5'-GGTCAGTCATGATTTCAATCAC-3' (reverse) designed from the nucleotide sequences in exons 3 and 4, respectively. For reference, mRNA levels of ß-actin were also evaluated using primers 5'-GACTTCGAGCAAGAG ATGGC-3' (forward) and 5'-AGGAAGGAAGGCTGG AAGAG-3' (reverse) designed from exon 4. Quantitative RT-PCR was performed on a SmartCycler (TaKaRa) using SYBR Green and analyzed with SmartCycler software ver.1.0 following the manufacturer's instruction. Relative amounts of *hnRNP A1* in each sample were calculated by dividing copy numbers of *hnRNP A1* transcripts with those for ß-actin. Precise evaluation of copy numbers of the transcripts was possible using standard curves generated with the known copy numbers of plasmid containing either *hnRNP A1* or ß-actin cDNA fragment amplified by the gene specific primers described above.

Statistical analysis. Statistical analysis was performed with the χ^2 or Kruskal-Wallis tests using an SPSS package (SPSS,

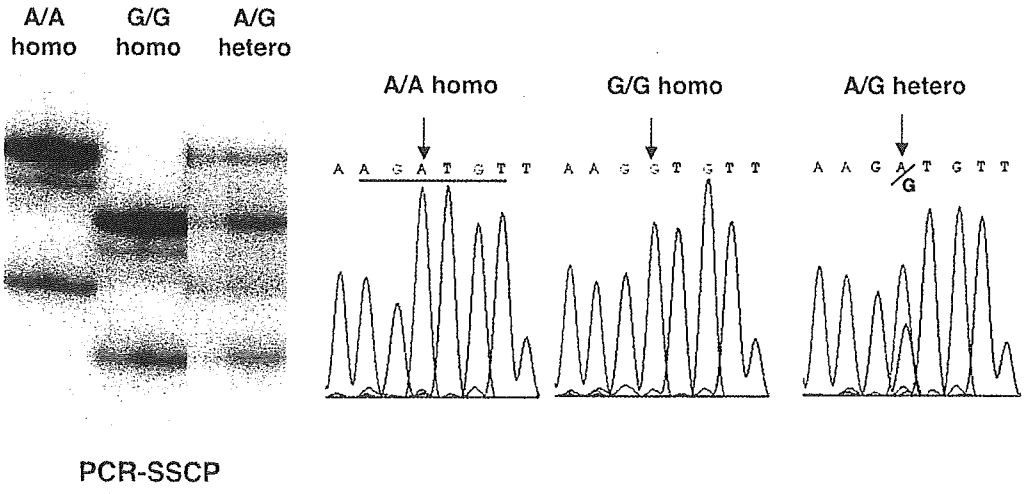

Figure 1. Single nucleotide polymorphism in the promoter region. PCR-SSCP analysis (left panel) shows three different patterns. Nucleotide sequencing analysis (right panel) reveals the presence of A/A and G/G homozygous alleles, and the A/G heterozygous allele. An underlined sequence is homologous to a putative recognition site for the GATA transcription factor proteins, being 5'-AGATCT-3'.

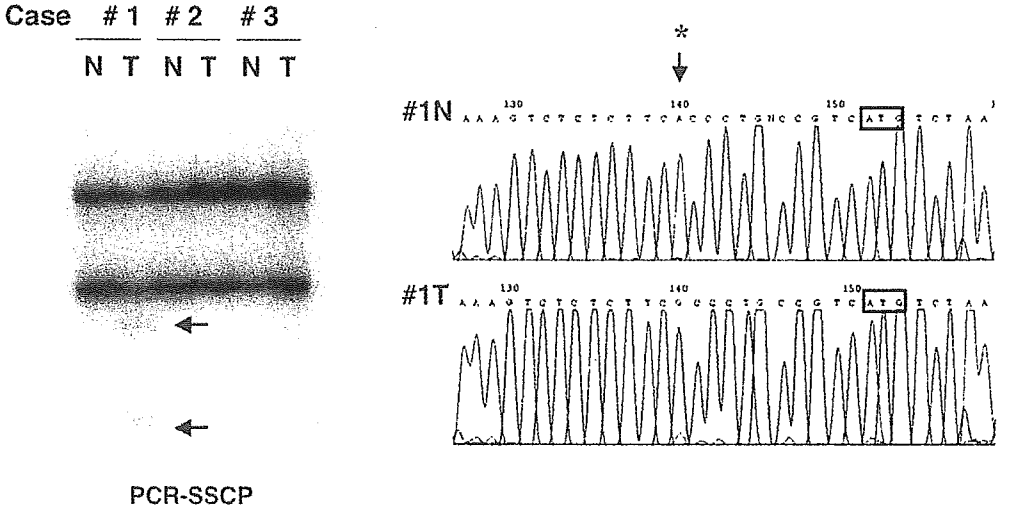

Figure 2. Mutation in the 5' non-coding region. PCR-SSCP analysis clearly reveals the presence of bands with altered mobility (left panel). Both bands were excised and DNA was extracted from the gel and amplified by PCR. Nucleotide sequencing of the amplified fragments was carried out using PCR-based direct sequencing. The asterisk (*) indicates an A to G transition-type base substitution at position -11 from the translation start site.

Japan) on a Macintosh computer. Student's t-tests were also carried out to determine the statistical significance of up-regulation of the gene at relatively early clinicopathological stages. Differences were considered significant when the P-value was <0.05.

Results

Single nucleotide polymorphism at the 5'-promoter region. Within the entire coding sequence of *hnRNP A1* and the 0.7 kbp 5'-promoter region, only one single nucleotide polymorphism (Fig. 1) was found by PCR-SSCP analysis among 30 patients, approximately 250 bp up-stream of the putative transcription start site. Three genotypes existed for this site, namely A/A (10/30) and G/G (8/30) homozygotes and the A/G heterozygote (12/30). Allele frequencies for 'A' and 'G' alleles were 53.3 and 46.7%, respectively, and the frequencies were almost comparable with those reported earlier according to the NCBI SNPs database (http://www.ncbi.nlm.nih.gov/entrez/query.fcgi). This polymorphism resides within a homologous sequence of a putative recognition site for the GATA transcription factor family (29,30).

hnRNP A1 somatic mutation at the 5'-UTR. The *hnRNP A1* gene encompasses approximately 4.5 kb, and is composed of 11 exons. We analyzed a 1,119 bp region of the entire coding sequence from exons 1 to 10 and 104 bp of 5'-UTR in exon 1 by PCR-SSCR analysis, and found only one case (case 1) with an A- to -G transition-type mutation at the -11 position from the translational initiation site (Fig. 2). No other mutations were found in the coding exons.

mRNA expression of hnRNP A1. Quantitative gene expression analysis revealed up-regulation of *hnRNP A1* in 18 (60%) of

cancer tissues by 2-fold or greater compared to their normal colon counterparts. In addition, one case in stage II demonstrated a 10-fold decrease of the expression in the cancer tissues. We further conducted correlation analysis between clinicopathological stages and fractions of cases with *hnRNP A1* overexpression. The percentages of cases demonstrating 2-fold or greater expression were 78% (7/9), 64% (7/11) and 40% (4/10) for stages II, III and IV, respectively, so that up-regulation of *hnRNP A1* was already observed from early stages. The difference between clinicopathological stages II and IV was not statistically significant by χ^2 analysis (P=0.096).

Discussion

From our present study, somatic mutations are very rare in the *hnRNP A1* in sporadic human colorectal cancers. Thus in 30 cases analyzed, we only found one with a point mutation in the 5'-UTR of exon 1. Furthermore, the mRNA expression in cancer tissue of this case was more than 6-fold elevated compared to the normal level. Although the biological significance of the mutation in the non-coding 5'-UTR is not clear yet, it may have affected the stability of the *hnRNP A1* mRNA and caused substantial increase in transcripts. Mutations in the 5'-UTR can modulate the translational efficiency, as in the case of *BRCA1* mutations in familial breast cancers (31).

Regarding the unique SNP in the promoter region, we do not have a clear idea whether this polymorphism might affect the constitutional level of *hnRNP A1* expression in the colorectal epithelium. A large-scaled population analysis needs to be conducted in the future to elucidate its biological significance for human colon carcinogenesis.

The main finding of the present study was frequent elevation in expression levels of *hnRNP A1* in colorectal cancer tissues. Such overexpression of *hnRNP* family genes has been reported in several types of cancers (32-36), and the *hnRNP A2/B1* gene is one of the best characterized gene, being up-regulated in human cancers, where it could serve as a biomarker for early detection of bronchial dysplasia and tumors in small sizes (32-34). Regarding the *hnRNP A1* gene, encoding one of the major hnRNPs and sharing a high sequence similarity with *hnRNP A2/B1*, only a few reports have so far been made regarding alterations of its expression in human cancers. Overexpression of *hnRNP A1* has previously reported in oligodendrogliomas (37) and in chronic myelogenous leukemias (38). In the latter case, interference with hnRNP A1 shuttling activity in myeloid progenitor cells resulted in a decrease of tumorigenic activity due to down-regulation of the anti-apoptotic factor Bcl-X_L (38).

At present, we do not have a definitive explanation of how high levels of *hnRNP A1* transcript might be implicated in colon carcinogenesis. One of the most plausible explanations is that high expression of the hnRNP A1 protein might be required for cancer cells to stably maintain the telomere repeats (24) because of their highly proliferative nature. If the replication fidelity of telomere repeats is abrogated or perturbed because of the presence of a higher structure in the G-rich repeats (22,23), it could be unfavorable for the fate of cancer cells. High levels of hnRNP A1 protein could resolve higher structures of G-rich repetitive sequences efficiently, improve the replication processibility of telomere DNA, and substantially enhance the survival of cancer cells. Alternatively, overexpression of *hnRNP A1* may have more active and direct influence, acting oncogenically in cells. Since variation in stoichiometry of hnRNP family proteins could affect cell-specific gene expression, as mentioned above (18), quantitative alteration of hnRNP A1 proteins could result in facilitation of malignant transformation of colon epithelial cells as a consequence of transcriptional and translational perturbation, as in BCR/ABL leukemogenesis (38). If this is the case, extremely low *hnRNP A1* expression in case 9 may have the same biological consequence as overexpression. In both cases, relative amounts of hnRNP family proteins would be altered, and this could perturb the translational machinery and contribute to neoplastic transformation, as mentioned above (19,38).

Lastly, it is also of great interest to note that overexpression of *hnRNP A1* was observed even in relatively early stages of colon carcinogenesis, in line with findings for bronchial hyperplasia during lung carcinogenesis (39). High expression of hnRNP A1 might thus be utilized as a surrogate marker for colorectal cancer screening as with hnRNP A2/B1 for human lung cancers, providing an additional informative biomarker for patients undergoing endoscopic examination.

Acknowledgements

We are grateful for Masako Ochiai and Ryoichi Masui for their technical assistance and critical comments throughout the manuscript. This work was supported in part by a Grant-in-Aid for the Second Term of the Comprehensive 10-Year Strategy for Cancer Control from the Ministry of Health, Labour and Welfare of Japan, and a Grant-in-Aid for Cancer Research from the Ministry of Health, Labour and Welfare of Japan.

References

1. Chung DC: The genetic basis of colorectal cancer: insights into critical pathways of tumorigenesis. Gastroenterology 119: 854-865, 2000.
2. Esteller M, Corn PG, Baylin SB and Herman JG: A gene hypermethylation profile of human cancer. Cancer Res 61: 3225-3229, 2000.
3. Notterman DA, Alon U, Sierk AJ and Levine AJ: Transcriptional gene expression profiles of colorectal adenoma, adenocarcinoma and normal tissue examined by oligonucleotide arrays. Cancer Res 61: 3124-3130, 2001.
4. Fujiwara K, Ochiai M, Ohta T, Ohki M, Aburatani H, Nagao M, Sugimura T and Nakagama H: Global gene expression analysis of rat colon cancers induced by a food-borne carcinogen, 2-amino-1-methyl-6-phenylimidazo[4,5-*b*]- pyridine. Carcinogenesis 25: 1495-1505, 2004.
5. Rajasekhar VK, Viale A, Socci ND, Widmann M, Hu X and Holland EC: Oncogenic Ras and Akt signaling contribute to glioblasoma formation by differential recruitment of existing mRNAs to polysomes. Mol Cell 12: 889-901, 2003.
6. Ruggero D, Montanaro L, Ma L, Xu W, Londei P, Cordon-Cardo C and Pandolfi PP: The translation factor eIF-4E promotes tumor formation and cooperates with c-Myc in lymphomagenesis. Nature Med 10: 484-486, 2004.
7. Clemens MJ: Targets and mechanisms for the regulation of translation in malignant transformation. Oncogene 23: 3180-3188, 2004.
8. Dreyfuss G, Kim VN and Kataoka N: Messenger-RNA-binding proteins and the messages they carry. Nat Rev Mol Cell Biol 3: 195-205, 2002.

9. Russell ID and Tollervey D: NOP3 is an essential yeast protein which is required for pre-rRNA processing. J Cell Biol 119: 737-747, 1992.
10. Piñol-Roma S and Dreyfuss G: Shuttling of pre-mRNA binding proteins between nucleus and cytoplasm. Nature 355: 730-732, 1992.
11. Mayeda A and Krainer AR: Regulation of alternative pre-mRNA splicing by hnRNP A1 and splicing factor SF2. Cell 68: 365-375, 1992.
12. Michelotti EF, Michelotti GA, Aronsohn AI and Levens D: Heterogeneous nuclear ribonucleoprotein K is a transcription factor. Mol Cell Biol 16: 2350-2360, 1996.
13. Izaurralda E, Jarmolowski A, Beisel C, Mattaj IW, Dreyfuss G and Fischer U: A role for the M9 transport signal of hnRNP A1 in mRNA nuclear export. J Cell Biol 137: 27-35, 1997.
14. Ostareck DH, Ostareck-Lederer A, Wilm M, Thiele BJ, Mann M and Hentze MW: mRNA silencing in erythroid differentiation: hnRNP K and hnRNP E1 regulate 15-lipoxygenase translation from the 3'-end. Cell 89: 597-606, 1997.
15. Collier B, Goobar-Larsson L, Sokolowski M and Schwartz S: Translational inhibition *in vitro* of human papillomavirus type heterogeneous ribonucleoprotein K and poly(rC)-binding proteins 1 and 2. J Biol Chem 273: 22648-22656, 1998.
16. Mayeda A, Helfman DM and Krainer AR: Modulation of exon skipping and inclusion by heterogeneous nuclear ribonucleoprotein A1 and pre-mRNA splicing factor SF2/ASF. Mol Cell Biol 13: 2993-3001, 1993.
17. Caceres JF, Stamm S, Helfman DM and Kraniner AR: Regulation of alternative splicing *in vivo* by overexpression of antagonistic splicing factors. Science 265: 1706-1709, 1994.
18. Kamma H, Portman DS and Dreyfuss G: Cell type-specific expression of hnRNP proteins. Exp Cell Res 221: 187-196, 1995.
19. Rosenwald IB: The role of translation in neoplastic transformation from a pathologist's point of view. Oncogene 23: 3230-3247, 2004.
20. Piñol-Roma S, Choi YD, Matunis MJ and Dreyfuss G: Immunopurification of heterogeneous nuclear ribonucleoprotein particles reveals an assortment of RNA-binding proteins. Genes Dev 2: 215-227, 1988.
21. Katahira M, Fukuda H, Kawasumi H, Sugimura T, Nakagama H and Nagao M: Intermolecular quadruplex formation of the G-rich strand of the mouse hypervariable minisatellite Pc-1. Biochem Biophys Res Commun 264: 327-333, 1999.
22. Enokizono Y, Matsugami A, Uesugi S, Fukuda H, Tsuchiya N, Sugimura T, Nagao M, Nakagama H and Katahira M: Destruction of quadruplex by proteins, and its biological implications in replication and telomere maintenance. Nucleic Acids Res 3 (Suppl): 231-232, 2003.
23. Fukuda H, Katahira M, Tsuchiya N, Enokizono Y, Sugimura T, Nagao M and Nakagama H: Unfolding of quadruplex structure in the G-rich strand of the minisatellite repeat by the binding protein UP1. Proc Natl Acad Sci USA 99: 12685-12690, 2002.
24. La Branche H, Dupuis S, Ben-David Y, Bani MR, Wellinger RJ and Chabot B: Telomere elongation by hnRNP A1 and a derivative that interacts with telomeric repeats and telomerase. Nature Genet 19: 199-202, 1998.
25. Fiset S and Chabot B: hnRNP A1 may interact simultaneously with telomeric DNA and the human telomerase RNA *in vitro*. Nucleic Acids Res 29: 2268-2275, 2001.
26. Beahrs OH, Henson DE, Hutter RVP and Kennedy BJ: Staging of cancer at specific anatomic sites. In: Manual for Staging of Cancer. 4th edition. Beahrs OH, Henson DE, Hutter RVP and Kennedy BJ (eds). Lippincott, Philadelphia, pp63-82, 1992.
27. Jass JR and Sobin LH: Definition and explanatory notes of stomach. In: Histological Typing of Intestinal Tumors. 2nd edition. Jass JR and Sobin LH (eds). Spinger-Verlag, Berlin, pp32-33, 1989.
28. Orita M, Iwahana H, Kanazawa H, Hayashi K and Sekiya T: Detection of polymorphisms of human DNA by gel electrophoresis as single-strand conformation polymorphisms. Proc Natl Acad Sci USA 86: 2766-2770, 1989.
29. Bai Y, Akiyama Y, Nagasaki H, Yagi OK, Kikuchi Y, Saito N, Takeshita K, Iwai T and Yuasa Y: Distinct expression of CDX2 and GATA4/5, development-related genes, in human gastric cancer cell lines. Mol Carcinogenesis 28: 184-188, 2000.
30. Ghirlando R and Trainor CD: Determinants of GATA-1 binding to DNA: the role of non-finger residues. J Biol Chem 278: 45620-45628, 2003.
31. Signori E, Bagni C, Papa S, Primerano B, Rinaldi M, Amaldi F and Fazio VM: A somatic mutation in the 5'UTR of BRCA1 gene in sporadic breast cancer causes down-modulation of translation efficiency. Oncogene 20: 4596-4600, 2001.
32. Sueoka E, Goto Y, Sueoka N, Kai Y, Kozu T and Fujiki H: Heterogeneous nuclear ribonucleoprotein B1 as a new marker of early detection for human lung cancers. Cancer Res 59: 1404-1407, 1999.
33. Fielding P, Turnbull L, Prime W, Walshaw M and Field JK: Heterogeneous nuclear ribonucleoprotein A2/B1 up-regulation in bronchial lavage specimens: a clinical marker of early lung cancer detection. Clin Cancer Res 5: 4048-4052, 1999.
34. Sueoka E, Sueko N, Goto Y, Matsuyama S, Nishimura H, Sato M, Fujimura S, Chiba H and Fujiki H: Heterogeneous nucler ribonucleoprotein B1 as an early biomarker for occult cancer of human lungs and bronchial dysplasis. Cancer Res 61: 1896-1902, 2001.
35. Gouble A, Grazide S, Meggetto J, Mercier P, Delsol G and Morello D: A new player in oncogenesis: AUF1/hnRNP D overexpression leads to tumorigenesis in transgenic mice. Cancer Res 62: 1489-1495, 2002.
36. Ostrowski J and Bomsztyk K: Nuclear shift of hnRNP K protein in neoplasms and other states of enhanced cell proliferation. Br J Cancer 89: 1493-1501, 2003.
37. Xu X, Joh HD, Pin S, *et al*: Expression of multiple largersized transcripts for several genes in oligodendrogliomas: potential markers for glioma subtype. Cancer Let 171: 67-77, 2001.
38. Iervolino A, Santilli G, Trotta R, Guerzoni C, Cesi V, Bergamaschi A, Gambacorti-Passerini C, Calabretta B and Perrotti D: hnRNP A1 nucleocytoplasmic shuttling activity is required for normal myelopoiesis and Bcr/Abl leukemogenesis. Mol Cell Biol 22: 2255-2266, 2002.
39. Pino I, Pio R, Toledo G, Zabalegui N, Vicent S, Rey N, Lozano M, Torre W, Garcia-Foncillas J and Montuenga LM: Altered pattens of expression of members of the heterogeneous nuclear ribonucleoprotein (hnRNP) family in lung cancer. Lung Cancer 41: 131-143, 2003.

Available online at www.sciencedirect.com
SCIENCE DIRECT®
ELSEVIER
Cancer Letters 220 (2005) 67–74
CANCER Letters
www.elsevier.com/locate/canlet

Differential staining of dysplastic aberrant crypt foci in the colon facilitates prediction of carcinogenic potentials of chemicals in rats

Masako Ochiai[a], Masatoshi Watanabe[b], Masako Nakanishi[a], Ayako Taguchi[a], Takashi Sugimura[a], Hitoshi Nakagama[a,*]

[a]*Biochemistry Division, National Cancer Center Research Institute, 5-1-1, Tsukiji, Chuo-ku, Tokyo 104-0045, Japan*
[b]*Laboratory for Medical Engineering, Division of Materials Science and Chemical Engineering, Graduate School of Engineering, Yokohama National University, 79-1 Tokiwadai, Hodogaya-ku, Yokohama 240-8501, Japan*

Received 2 September 2004; received in revised form 14 October 2004; accepted 15 October 2004

Abstract

We developed a novel and simple method to identify dysplastic aberrant crypt foci (ACF) induced in rats by colon carcinogens more efficiently and selectively without conducting laborious histological examination, which usually requires enough time to get final diagnosis. By adding a simple decolorization process with 70% methanol after conventional 0.2% methylene blue staining, dysplastic ACF could be differentially contrasted. To examine the validity of this novel method, which we refer to as differential staining, we analyzed colonic lesions induced by three heterocyclic amines, including 2-amino-1-methyl-6-phenylimidazo[4,5-*b*]pyridine, and found that the number of dysplastic ACF detected more precisely reflected their carcinogenic potential than the total numbers of ACF.

Keywords: PhIP; HCA; Dysplastic ACF; Differential staining; Colon carcinogenesis

1. Introduction

Rodent animal models have been widely utilized for research into different aspects of colon carcinogenesis, and have made a substantial contribution to the dissection of molecular bases of multi-stage development of colon cancer [1,2]. Aberrant crypt foci (ACF) were first reported by Bird et al. [3] as putative neoplastic lesions of the colon in mice treated with azoxymethane (AOM), and now are established biomarkers for rodent colon carcinogenesis. They have found particular application in medium-term evaluation of the carcinogenic or chemopreventive potential of environmental compounds [4], but conflicting evidence has also been presented and the biological significance of ACF is still controversial. For example, although hundreds of such lesions are induced in rats by AOM [5] and only a few by a food-borne carcinogen 2-amino-1-methyl-6-phenylimidazo[4,5-*b*]pyridine (PhIP) [6,7], the numbers of colon cancers induced by these two compounds are almost equal, at one or two per animal [5,8,9].

* Corresponding author. Tel.: +81 3 3547 5239; fax: +81 3 3542 2530.
E-mail address: hnakagam@gan2.res.ncc.go.jp (H. Nakagama).

0304-3835/$ - see front matter © 2005 Elsevier Ireland Ltd. All rights reserved.
doi:10.1016/j.canlet.2004.10.026

In addition, while some chemopreventive agents, such as 2-(carboxyphenyl)retinamide [10] or genistein [11, 12], effectively suppress ACF induction by AOM, they do not suppress or may even facilitate the development of colon cancers [10–12]. The most plausible explanation for the observed discrepancies is that ACF are in fact very heterogeneous in nature [13,14]. PhIP-induced ACF are histologically categorized into two types; namely, non-dysplastic and dysplastic ACF, the latter harboring *β-catenin* and/or *Apc* mutations, and demonstrating a mutation spectrum very similar to that observed in colon cancers. In contrast, mutations were rarely observed in non-dysplastic lesions. Other types of preneoplastic lesions may also exist and several candidates have been proposed as more relevant surrogate endpoints than ACF. These include β-catenin accumulated crypts [15], mucin-depleted foci [16] and microadenomatous lesions in the Apc^{Min} mouse [17]. However, whether these overlap with dysplastic ACF has remained unclear. One difficulty is that their identification has hitherto relied on laborious histological examination of very tiny lesions embedded in colon epithelium, which usually requires enough time to get final diagnosis.

In the present study, we therefore focused on a novel and simple method to identify dysplastic types of ACF in an efficient and selective manner. Using this novel approach, numbers of dysplastic ACF induced by different heterocyclic amines (HCAs), including PhIP, were determined to assess their correlation with colon carcinogenic potential evaluated from the long-term studies of tumor development.

2. Materials and methods

2.1. Animals, diet and heterocyclic amines

Five-week-old Fischer344 (F344) male rats were purchased from CLEA Japan (Tokyo, Japan). Three HCAs, namely PhIP, 2-amino-3,4-dimethylimidazo[4,5-*f*]quinoline (MeIQ), and 2-amino-3-methylimidazo[4,5-*f*]quinoline (IQ) were obtained from the Nard Institute (Osaka, Japan), and mixed in AIN-93G diet (Dyets, Bethlehem, PA) at concentrations of 400, 300 and 300 ppm, respectively; doses which have been previously used for long-term carcinogenesis studies of HCAs [18].

2.2. Animal experiments

F344 male rats were housed in wire cages in an air-conditioned room at 25 °C with a 12 h cycle of light and dark. After a 1-week acclimatization to the housing environment, the animals were given free access to AIN-93G diet containing PhIP (400 ppm), MeIQ (300 ppm) or IQ (300 ppm), following our intermittent HCA-feeding protocol in combination with a high fat diet (Dyets) as described previously [13]. Controls received the same diet without HCAs. All animals were sacrificed at week 32, and subjected to histological and genetic analysis of induced ACF and colon tumors. The experiments were conducted according to the 'Guidelines for Animal Experiments in National Cancer Center, Japan'.

2.3. Conventional methylene blue staining of ACF

The colons were resected, cut open along the longitudinal median axis, and submerged in 10% neutralized formalin overnight at 4 °C. They were then cut equally into four lengths from the proximal to the distal ends, and stained with 0.2% methylene blue in PBS as described elsewhere [3]. ACF detected with this conventional methylene blue staining at this point are referred to hereafter as 'conventional ACF'.

2.4. Differential staining of ACF

Strips of colon tissues stained as above were subsequently decolorized with 70% methanol with gentle shaking at room temperature for 4–6 min, and ACF, which retain staining, were re-counted. Note that 'ACF' hereafter means ACF detected after this decolorization process, and are discriminated from conventional ACF. We also refer to this novel staining method as the 'differential staining method' since a subset of ACF thereby could be clearly detected, as detailed below. Digital images of stained lesions were captured by a Charge Coupled Device (CCD) camera (HC-2500, Fuji Film Co, Ltd, Tokyo), modified by Adobe Photoshop (Macintosh, Adobe Systems, CA), and stored as Tagged Image File Format (TIFF, Macintosh) files.